

Entanglement revivals as a probe of scrambling in finite quantum systems

Ranjan Modak,¹ Vincenzo Alba,² and Pasquale Calabrese^{1,3}

¹*SISSA and INFN, via Bonomea 265, 34136 Trieste, Italy*

²*Institute for Theoretical Physics, Universiteit van Amsterdam,
Science Park 904, Postbus 94485, 1098 XH Amsterdam, The Netherlands*

³*International Centre for Theoretical Physics (ICTP), Strada Costiera 11, 34151 Trieste, Italy*

The entanglement evolution after a quantum quench became one of the tools to distinguish integrable versus chaotic (non-integrable) quantum many-body dynamics. Following this line of thoughts, here we propose that the revivals in the entanglement entropy provide a finite-size diagnostic benchmark for the purpose. Indeed, integrable models display periodic revivals manifested in a dip in the block entanglement entropy in a finite system. On the other hand, in chaotic systems, initial correlations get dispersed in the global degrees of freedom (information scrambling) and such a dip is suppressed. We show that while for integrable systems the height of the dip of the entanglement of an interval of fixed length decays as a power law with the total system size, upon breaking integrability a much faster decay is observed, signalling strong scrambling. Our results are checked by exact numerical techniques in free-fermion and free-boson theories, and by time-dependent density matrix renormalisation group in interacting integrable and chaotic models.

I. INTRODUCTION

Integrable and chaotic many-body quantum systems are very different objects. The former have infinite classes of local charges constraining their dynamics; conversely, the latter have only few local integrals of motion. Integrable systems admit stable quasiparticles with infinite lifetime and elastic scattering between them [1]. When non-integrable models have some quasiparticles at all, they have a finite lifetime and inelastic scattering with particles production. One would then expect their unitary non-equilibrium dynamics (say following a quantum quench [2]) to be completely different [3]. Indeed, it is nowadays well established that while chaotic systems long time after a quench are described by the Gibbs (thermal) ensemble [4–11], an integrable system fails to thermalise and a statistical description of its asymptotic local properties requires a Generalised Gibbs Ensemble (GGE) [12–44], which takes into account all the local and quasilocal conserved quantities of the system [30, 31, 44]. However, there are many cases when the predictions from GGE and thermal ensembles are too close to each other. Furthermore, an integrable point constrains the dynamics of a relatively large neighbourhood in parameter space, giving rise to the phenomenon of prethermalisation, according to which only for extremely large times the thermal behaviour is attained, while at accessible times one observes a quasi-stationary state with quasi-integrable features [45–53].

These observations were among those that initiated the search for concepts that naturally take integrable and chaotic models apart. A very suggestive proposal concerns the *scrambling of quantum information*, hence of entanglement. Indeed, qualitatively we expect that in integrable systems the spreading of entanglement, due to the quasiparticles with a local-in-space structure, happens in a “localised” manner, i.e., local initial correlations are somewhat preserved. This is the essence of the quasiparticle picture for entanglement spreading [54–57]. This scenario must change in non-integrable models: the common lore is that inelastic processes and the quasiparticle decay should facilitate the delocalisation of the initial correlation in the global degrees of freedom of the system [58–67]. This idea originated in the context of the black-hole information paradox [68–70]. There the initial correlation between the interior and the exterior of the black hole gets dispersed in the global degrees of freedom of the radiation that remains after the black hole evaporates.

Unfortunately, probing the scrambling scenario in microscopic quantum many-body systems proved to be a daunting task. Several diagnostic tools have been devised, such as the tripartite mutual information [71, 72], out-of-time-ordered correlators [70], and operator space entanglement entropy [73–75]. An idea that is related to this paper is to diagnose scrambling from the time evolution of the mutual information between two disjoint intervals. Indeed, in integrable models, because of the infinite lifetime of the quasiparticles, the mutual information exhibits a peak at intermediate times, as first pointed out in conformal field theory (CFT) [54]. For chaotic systems, due to scattering and finite lifetime of quasiparticles, the peak should decay, signalling scrambling. This behaviour has been first proposed and observed in CFTs with large central charge [76–79] and better characterised for integrable systems with non-linear dispersion in Ref. [80].

It is of fundamental importance to devise further diagnostic tools to probe quantum information scrambling. Here, we propose and show that entanglement revivals in finite systems can be used for this purpose. The idea to use revival effects to distinguish between ergodic and non-ergodic systems has already been explored in Refs. [81, 82], but in different contexts. Revivals have been studied in Conformal Field Theory [83, 84] (see Ref. 85 and 86 for

some comparison with lattice realisations). Nevertheless, the inspiration for our work came from recent results for maximally chaotic models in which the entanglement entropy shows no revivals at all in finite size [88–90], while in the integrable limit a perfect recurrence is observed. These results are the two black and white extremes of a more refined and grey structure which we investigate and characterise here.

Our main result is that it is possible to detect scrambling by monitoring the first entanglement revival. We consider a subsystem of fixed size ℓ embedded in a system of finite size L . We consider initial product states, i.e., with zero entanglement entropy. For time $t \lesssim \ell$ the entropy increases linearly. At larger times $\ell \ll t \lesssim L$ the entropy saturates. At the first revival time $t = t_R \propto L$, the entanglement entropy decreases, and it exhibits a dip, which is followed by a later increase. As L increases the revival time $t_R \propto L$ is shifted to longer times and the height of the dip decreases. We show that for integrable systems the dip decays algebraically in L (as $L^{-1/2}$ within the quasiparticle picture), as we explicitly test in free-fermion, free-boson, and interacting integrable models. Remarkably, upon breaking integrability, the dip exhibits a much faster decay, signalling strong scrambling.

A main observation concerns the comparison with the mutual information, which is a very similar diagnostic tool for scrambling that two of us proposed in Ref. 80. For the entanglement revival we require only to calculate the single interval entanglement entropy, which in the framework of Matrix Product States (MPS) is much easier and less numerically demanding than the entanglement entropy of two intervals required for the mutual information. As a drawback, we need to explore times growing linearly with L and, depending on circumstances, such times can be harder than those required for the mutual information that must grow linearly with the separation of the two intervals. At the end of the day, we believe that the combined use of the two tools provides a rather clear indication of the integrability/chaotic nature of the model under scrutiny.

The paper is organised as follows. In Sec. II we introduce the scrambling of entanglement revivals in integrable models within the quasiparticle picture. In Secs. III and IV we work out explicit predictions and test them for free-fermion and free-boson models, respectively. In Sec. V we move to interacting integrable models focusing on the Heisenberg spin chain and a numerical study of its quench dynamics by means of time-dependent Density Matrix Renormalisation Group (tDMRG) techniques. In section VI we discuss the effects integrability breaking on the entanglement revivals. Our conclusions are in section VII.

II. SCRAMBLING AND ENTANGLEMENT REVIVALS IN INTEGRABLE MODELS

The typical protocol to drive a system out of equilibrium is the *quantum quench* [2]: an isolated system is initially prepared in a non-equilibrium pure state $|\psi_0\rangle$ and then it is let evolve under the unitary dynamics governed by a Hamiltonian H . Although the dynamics is unitary and the entire system remains in a pure state, at long times the reduced density matrix ρ_A of an arbitrary finite compact subsystem A of length ℓ displays local thermodynamic equilibrium. The reduced density matrix ρ_A is defined as

$$\rho_A \equiv \text{Tr}_B |\psi(t)\rangle\langle\psi(t)|, \quad (1)$$

where the trace is over the degrees of freedom of the complement B of A , and $|\psi(t)\rangle \equiv e^{-iHt}|\psi_0\rangle$ is the time-dependent state of the system. Local thermal equilibrium means that ρ_A for large times equals the reduced density matrix of a statistical ensemble [41].

A key question is how entanglement spreads in out-of-equilibrium many-body system, both theoretically and experimentally, thanks to recent progress on the direct measurement of entanglement dynamics with cold atoms and trapped ions [91–97]. One of the most useful entanglement measures is the von Neumann (entanglement) entropy [98]

$$S_\ell \equiv -\text{Tr} \rho_A \ln \rho_A. \quad (2)$$

Here we are interested in the out-of-equilibrium dynamics of S_ℓ after a quantum quench. Our main result is that the dynamics of S_ℓ in finite-size systems depends dramatically on whether the Hamiltonian is integrable or chaotic.

To understand why this is the case, let us first briefly describe the quasiparticle picture for the entanglement spreading which is applicable to generic integrable models (first introduced in Ref. [54] in the context of CFT). According to this picture, the initial state acts as a source of quasiparticle excitations which are produced in *pairs* and uniformly in space. After being created, the quasiparticles move ballistically through the system with opposite velocities. Only quasiparticles created at the same point in space are entangled and while they move far apart they carry entanglement and correlation in the system. A pair contributes to the entanglement entropy at time t only if one particle of the pair is in A (the interval of length ℓ) and its partner in B . Keeping track of the linear trajectories of the particles, it is easy to conclude [54, 55]

$$S(t) = \sum_n \left[2t \int_{|v_n|t < \ell} dk v_n(k) s_n(k) + \ell \int_{|v_n|t > \ell} dk s_n(k) \right]. \quad (3)$$

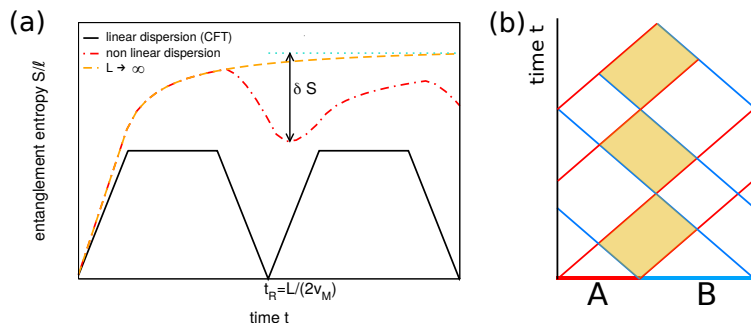


FIG. 1. (a) Schematic diagram of entanglement dynamics for finite-size integrable systems. The continuous line is the quasiparticle prediction for a model with exactly linear dispersion, such as a CFT. Note the perfect revival at t_R . The dashed-dotted line is the quasiparticle prediction for a model with a realistic nonlinear dispersion. For $L \rightarrow \infty$ the entropy saturates (dashed line), while at finite size (dot-dashed line) it shows a dip of height δS , which is the main quantity we consider. The precise definition of δS is shown pictorially as the difference between the asymptotic result for infinite systems ($S_\ell(\infty)$, dot line) and the minimum of the entropy close to the first revival. (b) Pictorial interpretation of (4). The slanted lines are the trajectories of the entangled quasiparticles created at the interface between the two subsystems. At a given time t , the entanglement entropy is proportional to the horizontal section of the shaded region at that time. Three revivals are explicitly shown. The quasiparticles turn around the system because of periodic boundary conditions

Here the sum is over the species of particles n whose number depends on the model, k represents their quasimomentum (rapidity), $v_n(k)$ is their velocity, and $s_n(k)$ their contribution to the entanglement entropy. (Often we will work with a single species of quasiparticle omitting the sum over n and the subscripts). The quasiparticle prediction (3) for the entanglement entropy holds true in the space-time scaling limit, i.e. $t, \ell \rightarrow \infty$ with the ratio t/ℓ fixed. When a maximum quasiparticle velocity v_M exists (e.g., as a consequence of the Lieb-Robinson bound [99]), Eq. (3) predicts that for $t \leq \ell/(2v_M)$, S_ℓ grows linearly in time. Conversely, for $t \gg \ell/(2v_M)$, only the second term survives and the entanglement is extensive in the subsystem size, i.e., $S_\ell \propto \ell$. In order to give predictive power to Eq. (3), one should fix the values of $v_n(k)$ and $s_n(k)$: the former are the group velocities of the excitations around the stationary state [55, 56, 100] and the latter are the thermodynamic entropy densities of the GGE [55, 56]. The validity of Eq. (3) has been carefully tested both analytically and numerically in free-fermion and free-boson models [54, 101–113] and in many interacting integrable models [55, 56, 114–118]. The mechanism for the entanglement evolution in chaotic systems is different, not as well understood as in integrable models and with many peculiar features. Nevertheless, the entanglement entropy grows linearly up to a time extensive in subsystem size [88–90, 119–126], exactly as in integrable systems.

Interestingly, Eq. (3) has been generalised to capture the non-equilibrium dynamics in many different physical situations and to other physical quantities. For example we mention quenches from inhomogeneous initial states [127–134] and states with more complicated quasiparticle structure than simple uncorrelated pairs [135–137]. Furthermore, the picture has been adapted to describe the steady-state Rényi entropies [138–141] and to the dynamics of the logarithmic negativity [142–144]. Very recently, it has been shown that by using the quasiparticle picture it is also possible to study the fate of the entanglement in free-fermion systems in the presence of dissipation [145] (see also Ref. 146). An aspect that is of much importance for our analysis is the behaviour of the mutual information between two disjoint intervals [80]. In integrable systems, the mutual information exhibits an algebraic decay with the distance between the intervals, that within the quasiparticle picture has a decay exponent equal to 1/2. Away from the scaling limit, the power-law behaviour persists, but with a larger (and model-dependent) exponent. For non-integrable models, a much faster decay, compatible with an exponential, is observed.

We recall that in Eq. (3) we assume that subsystem A of length ℓ is embedded in an infinite system. The result is different for a finite system of total length L in which, as we are going to show, the entanglement entropy exhibits revivals (we focus on periodic boundary conditions, but other boundary conditions lead just to minor adjustments as long as they are compatible with integrability; indeed we will later turn to open boundary conditions too). We assume that L is large enough so that quasiparticles are well-defined; this implies that the space-time scaling limit generalises as $t, \ell, L \rightarrow \infty$ with both t/ℓ and ℓ/L fixed (or, equivalently, t/L). At this point, to study the revivals we need to modify Eq. (3), simply accounting for the quasiparticles trajectories in a periodic system.

Let us start by describing what happens when all quasiparticles have the same velocity v regardless of momentum, as it is the case, e.g., in CFT. The entropy first grows linearly up to $\ell/(2v)$. Then, it exhibits a plateau. Up to this time, the entanglement behaves like in an infinite system. The plateau terminates at $t = (L - \ell)/(2v)$ when the first quasiparticles produced at one boundary of the subsystem re-enter into it from the other edge after having turned around the circle. After this time, more and more quasiparticles will re-enter the subsystem producing a drop of the

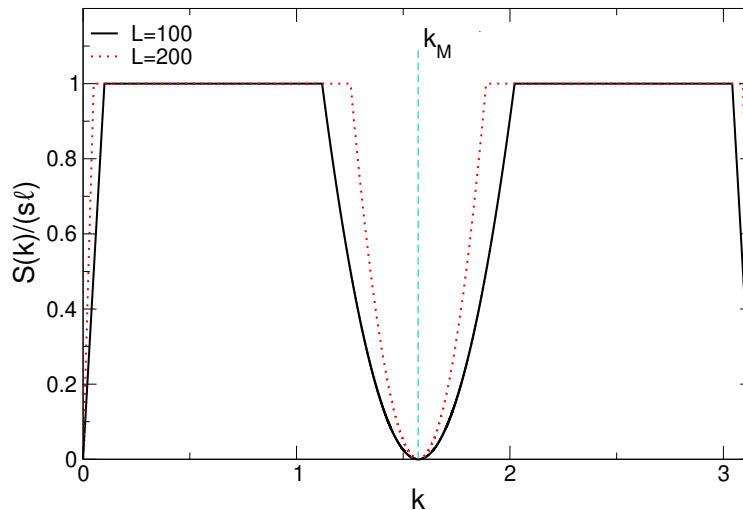


FIG. 2. Physical mechanism for the vanishing of the entanglement revivals in integrable systems. The figure shows the contribution of the quasiparticles to the density of entanglement entropy $S(k)/(s\ell)$ at the revival time $t = L/(2v_M)$ plotted versus their quasimomentum k . Here we consider quasiparticles with group velocity $v(k) = \sin(k)$, assuming $S(k)/\ell = s$, with s a constant. The entropy density is obtained by integrating over k . In the limit $L \rightarrow \infty$ with finite subsystem size ℓ all the quasiparticles contributions are present, i.e., $S(k)/(s\ell) = 1$ for any k . At finite L the contributions due to slow quasiparticles (with $k \approx 0$ and $k \approx \pi$) and quasiparticles with maximum velocity at $k \approx k_M$ are suppressed (dips in the figure). This gives rise to the dip in Fig. 1 (a). Note that in the limit $L \rightarrow \infty$ the size of the dips due to the missing quasiparticles shrinks, reflecting the vanishing of the entanglement revival. Note also that the entanglement revival is dominated by quasiparticles with maximum velocity.

entropy that lasts until the *revival time* $t_R = L/(2v)$, when the dynamics restart exactly like if the system was at $t = 0$. And so on in a periodic fashion in time. This entropy dynamics is shown in Fig. 1 (a) as a full line. The physical origin of the entanglement revivals is illustrated in Fig. 1 (b), focusing on the trajectories of the quasiparticles. To understand the entanglement dynamics is sufficient to consider the trajectories of the entangled quasiparticles created at the interfaces between A and B (slanted lines in Fig. 1 (b)). Note that in the figure we use periodic boundary conditions. It is clear that at a given time t the number of entangled pairs that are shared between A and B , and hence the entanglement entropy, is proportional to the horizontal section at that time of the shaded area in the figure.

Taking into account the different velocities $v(k)$ of the quasiparticles is now trivial: it is enough to sum/integrate over all possible quasi-momenta k the result for each mode. For the case of a single species of quasiparticles, one obtains

$$S_\ell(t) = \int_{\left\{\frac{2v(k)t}{L}\right\} < \frac{\ell}{L}} \frac{dk}{2\pi} s(k)L \left\{ \frac{2v(k)t}{L} \right\} + \ell \int_{\frac{\ell}{L} \leq \left\{\frac{2v(k)t}{L}\right\} < 1 - \frac{\ell}{L}} \frac{dk}{2\pi} s(k) + \int_{1 - \frac{\ell}{L} \leq \left\{\frac{2v(k)t}{L}\right\}} \frac{dk}{2\pi} s(k)L \left(1 - \left\{ \frac{2v(k)t}{L} \right\} \right), \quad (4)$$

where $\{x\}$ denotes the fractional part of x , e.g., $\{1.76\} = 0.76$. This result has been already reported in Ref. [147] (suggested by one of the present authors, as acknowledged there), but in a different context. The structure of Eq. (4) is the same as Eq. (3): $s(k)$ is the thermodynamic entropy of the GGE that describes the steady state, and $v(k)$ are velocities of the low-lying excitations around the corresponding thermodynamic macrostate. Taking into account the existence of more species trivially amounts to sum also over the different species, each with its own velocity and entropy density in momentum space, in full analogy to Eq. (3).

We now discuss the time evolution of S_ℓ for fixed ℓ, L as predicted by Eq. (4), for systems with nonlinear quasiparticles dispersion. The qualitative behaviour is shown as a dashed-dotted line in Fig. 1 (a). The entropy grows linearly up to $\ell/(2v_M)$, where now v_M is the maximum quasiparticles velocity. Importantly, in a realistic quantum many-body system there is a continuum of excitations with different velocities. This implies that the “plateau” in Fig. 1 (a) at $\ell/(2v_M) \ll t \lesssim (L - \ell)/(2v_M)$ is not flat but shows a slow saturation in the limit $L \rightarrow \infty$. Such slow saturation terminates at $t = (L - \ell)/(2v_M)$. After the most important aspect for our purposes comes: at $t = t_R \equiv L/(2v_M)$ the entropy exhibits a *partial revival*, in contrast to the case with a single velocity when the revival is perfect. The reason for this partial revival is obvious: when the fastest quasiparticles do not entangle anymore A and B because the pairs

are back to their original position, there are still many slow quasiparticles that are still contributing to S_ℓ . Here we focus on the dip in the entanglement entropy at (or close to) $t = t_R$. We consider the scaling for large L at fixed ℓ (which is still considered large enough for the quasiparticle picture to apply), i.e., we work in the regime $t, \ell, L \rightarrow \infty$ with t/ℓ and t/L fixed but $\ell \ll L$. (If we had considered the limit with ℓ/L of order 1, we would have approached a scaling curve for large L .) See below for a discussion about the applicability of these limits. The dip at t_R becomes less and less pronounced as L gets larger (at fixed ℓ), because more and more quasiparticles do not have time to reach the subsystems after going around the circle. To quantify this effect, we consider the (normalised) height δS of the dip (see Fig. 1 (a)), which is measured with respect to the saturation value of the entropy in the infinite system as

$$\delta S \equiv \frac{S_\ell(\infty) - S_\ell(t_R)}{\ell}, \quad \text{with} \quad S_\ell(\infty) \equiv \lim_{t \rightarrow \infty} \lim_{L \rightarrow \infty} S_\ell(t). \quad (5)$$

The definition of δS is illustrated pictorially in Fig. 1 (a).

We now discuss the behaviour of δS in the framework of the quasiparticle picture. We consider a generic integrable quantum many-body systems, with a continuum of entangling quasiparticles. Since we focus on the first revival at $t_R = L/(2v_M)$, we replace $t \rightarrow t_R$ in Eq. (4), which yields

$$S_\ell(t = t_R) = \int_{\frac{v(k)}{v_M} < \frac{\ell}{L}} \frac{dk}{2\pi} s(k) L \frac{v(k)}{v_M} + \ell \int_{\frac{\ell}{L} \leq \frac{v(k)}{v_M} < 1 - \frac{\ell}{L}} \frac{dk}{2\pi} s(k) + \int_{1 - \frac{\ell}{L} \leq \frac{v(k)}{v_M}} \frac{dk}{2\pi} s(k) L \left(1 - \frac{v(k)}{v_M}\right). \quad (6)$$

We now show that Eq. (6) implies that δS (cf. (5)) scales like $\delta S \propto L^{-1/2}$ for $L \rightarrow \infty$. In fact, in the limit $L \rightarrow \infty$ (i.e. $L \gg \ell$), the dip of the entanglement entropy, as discussed above, is dominated by the quasiparticles with $v \approx v_M$ (slowest quasiparticles did not have time to go around the system). This is illustrated in Fig. 2. In the figure we plot the quasiparticles contributions to the entropy density S/ℓ at the revival time $t = L/(2v_M)$ versus the momentum of the quasiparticles k . The result is obtained by using (4). We restrict to quasimomenta in $[0, \pi]$ because the entropy is an even function of k . For simplicity we assume that $s(k) = s$ (cf. (4)) for any k and $v(k) = \sin(k)$. In the limit $L \rightarrow \infty$ all the quasiparticles contribute to the entropy. This corresponds to the the plateaux at $t \rightarrow \infty$ in Fig. 1 (a). For finite L the contributions of the slow quasiparticles at $k \approx 0, \pi$ and of the quasiparticles with maximum velocity $v_M = v(k_M)$ are suppressed. This manifest itself in the dips at $k \approx k_M$ and $k \approx 0, \pi$. This gives rise to the dip at the time of the entanglement revival in Fig. 1 (a). Importantly, upon increasing L the dips in Fig. 2 (a) shrink, which correspond to the vanishing of the entanglement revival. Note that the leading contribution in powers of $1/L$ originates from the fast quasiparticles with $v \approx v_M$, whereas the contribution of slow ones with $k \approx 0, \pi$ is subleading.

Therefore, we expand the velocity of quasiparticle $v(k)$ around k_M (the momentum with maximum velocity, $v_{k_M} = v_M$) up to second order in $k - k_M$ as

$$\frac{v(k)}{v_M} = 1 - \frac{v''}{2v_M} (k_M - k)^2 + o(k_M - k)^3, \quad \text{with} \quad v'' \equiv -\frac{\partial^2 v(k)}{\partial k^2} \Big|_{k=k_M}. \quad (7)$$

If there are more momenta with maximum velocity, we should just sum over them. We assume that the entanglement content of the quasiparticles $s(k)$ is such that $s(k) = s_M + o(1)$ with a nonzero $s_M \equiv s_{k_M}$. Plugging these expansions in Eq. (6), we obtain

$$S_\ell(t_R) = S_\ell(\infty) - \frac{4}{3\pi} \left(\frac{2v_M}{v''}\right)^{1/2} \left(\frac{\ell}{L}\right)^{1/2} s_M \ell + \ell O\left(\frac{\ell}{L}\right), \quad (8)$$

where $S_\ell(\infty)$ is the asymptotic value of entanglement entropy in the thermodynamic limit, cf. Eq. (5). Few comments are needed. First of all, we only considered one species of quasiparticles, but for the validity of Eq. (8) this is unimportant: when there are more types of quasiparticles, these have well separated maximum velocities and so for large ℓ and L only one matters and Eq. (8) remains valid. However, the different species of quasiparticles can give strong finite size effects, as we shall see. Second, we note that Eq. (8) has the same structure as the formula describing the decay of the mutual information peak between two far apart intervals that has been derived in Ref. [80] and indeed has the same physical origin. Finally, let us stress the main limitation of Eq. (8). We obtained it in the quasiparticle picture in the limit $\ell/L \rightarrow 0$. However, this is not fully justified because the quasiparticle picture is valid for ℓ/L fixed and finite. Still, we can think of the limit in which $\ell = aL$ with $a \ll 1$. Thus, we expect the quasiparticle picture to describe an intermediate regime between very small ℓ (in which ℓ/L is not of order 1) and the scaling regime with ℓ of the same order of L . We recall that this is exactly what it has been found for the mutual information peak in [80]. There is not a general approach to understand the scaling for very small ℓ since it is expected to be model dependent; for example, from the analogous result of the mutual information peak [80], we would expect for free fermion the dip to decay as $L^{-2/3}$ while for free bosons as L^{-1} .

We want finally to comment on another interesting aspect of Eq. (8). If we expanded for large L and at fixed ℓ , the quasiparticle prediction for the entanglement evolution (6) at any time away from the revivals, we would trivially obtain an analytic behaviour in L^{-1} , because the velocity, away from the maximum has a linear term in k . In this respect, the non-analytic scaling at the revival time is a straightforward consequence of expanding close to an extreme of the velocity (exactly like in Landau-Ginzburg approach, the mean field exponent 1/2 is caused by expanding close to the minimum of the free energy).

In the following section, we numerically verify Eq. (8) in free-fermion and free-boson models, as well as in interacting integrable models. We will show how for small ℓ there is a crossover towards another power-law scaling. Finally, we will provide numerical evidence that in non-integrable models the dip of the entanglement revival decays faster than algebraically (likely exponentially).

III. FREE FERMIONS

In this section focus on the XY chain that can be mapped to a free-fermion model. The XY spin chain with a transverse magnetic field has Hamiltonian

$$H = - \sum_{j=1}^L \left[\frac{1+\gamma}{2} \hat{S}_j^x \hat{S}_{j+1}^x + \frac{1-\gamma}{2} \hat{S}_j^y \hat{S}_{j+1}^y + h \hat{S}_j^z \right], \quad (9)$$

where \hat{S}_i^α are spin-1/2 operators acting at site i , γ is the anisotropy, h the transverse field, and we use periodic boundary condition. The Hamiltonian (9) can be diagonalized by a combination of Jordan-Wigner, Fourier transform, and Bogoliubov transformations, leading to the free fermion model [148]

$$H = \sum_k \epsilon_k \hat{c}_k^\dagger \hat{c}_k, \quad \text{with} \quad \epsilon_k^2 = (h - \cos k)^2 + \gamma^2 \sin^2 k, \quad (10)$$

and \hat{c}_k are standard spinless fermionic ladder operators. The quasiparticle velocity is $v(k) = d\epsilon_k/dk$. Note that the quasiparticles' velocities do not depend on the initial state because the system is non-interacting. However, the initial state determines the structure of the entangling quasiparticles produced after the quench, and hence the velocity at which entanglement spreads (see, for instance, Ref. 135 and 87). Clearly, the velocities depend on the initial state in the presence of interactions [55, 100].

Here we consider a quench of the magnetic field h and of γ . Precisely, the system is initially prepared in the ground state of (9) with magnetic field h_0 and γ_0 . Then, the parameters are suddenly changed as $h_0 \rightarrow h$ and $\gamma_0 \rightarrow \gamma$. The quench is parametrised in terms of the difference of the Bogoliubov angles of pre- and post-quench Hamiltonians, i.e. [54, 101, 149]

$$\cos \Delta_k = \frac{hh_0 - \cos k(h + h_0) + \cos^2 k + \gamma\gamma_0 \sin^2 k}{\epsilon\epsilon_0}, \quad (11)$$

where ϵ_0, ϵ stand for pre- and post-quench dispersion relations (see Eq. (10)).

The GGE built with local conservation laws for the Hamiltonian (9) is equivalent [19, 26] to the one built with mode occupation numbers $\hat{n}_k = \hat{c}_k^\dagger \hat{c}_k$ and it is convenient to work with the latter. The GGE density matrix is then [19, 26]

$$\rho_{\text{GGE}} = \frac{e^{-\sum_k \lambda_k \hat{n}_k}}{Z}, \quad (12)$$

where $Z = \text{Tr} e^{-\sum_k \lambda_k \hat{n}_k}$ ensures the normalization $\text{Tr} \rho_{\text{GGE}} = 1$. The Lagrange multipliers λ_k are fixed by imposing that the expectation value of \hat{n}_k in the initial state coincides with its GGE prediction

$$\langle \hat{n}_k \rangle_{\text{GGE}} = - \frac{\partial}{\partial \lambda_k} \sum_p \ln(1 + e^{-\lambda_p}) = \frac{1}{1 + e^{\lambda_k}}. \quad (13)$$

Now λ_k is obtained requiring that $\langle \hat{n}_k \rangle_{\text{GGE}} = \langle \psi_0 | \hat{n}_k | \psi_0 \rangle = n_k$. The thermodynamic entropy of the GGE is the thermodynamic entropy obtained from the occupation n_k , which reads

$$S_{\text{GGE}} = -\text{Tr} [\rho_{\text{GGE}} \ln \rho_{\text{GGE}}] = \sum_k -n_k \ln n_k - (1 - n_k) \ln(1 - n_k) = \sum_k s(k), \quad (14)$$

where, $s(k) = -n_k \ln n_k - (1 - n_k) \ln(1 - n_k)$ is identified as the entropy contribution of the quasiparticle with momentum k .

In terms of (11), we have $n_k = \frac{1 + \cos \Delta_k}{2}$ and so the quasiparticles entanglement content $s(k)$ reads

$$s(k) = -\frac{1 + \cos \Delta_k}{2} \ln \left(\frac{1 + \cos \Delta_k}{2} \right) - \frac{1 - \cos \Delta_k}{2} \ln \left(\frac{1 - \cos \Delta_k}{2} \right). \quad (15)$$

The quasiparticle prediction for the entanglement entropy for a quench in the XY chain is obtained by plugging this value of $s(k)$ and $v(k) = v_M \sin k$ in Eq. (4). This time evolution (in the thermodynamic limit) has been also confirmed by ab initio approach both on the lattice [101] and in the field theory limit [150].

A. A special case: The Néel quench in the XX chain

There is a special case of the quench above that we want to discuss separately because it will be important for the generalisation to interacting (both integrable and not) fermionic model. This is the time evolution starting from the Neel state (in the z direction) and evolving with the isotropic XX Hamiltonian. This quench just amounts to take the limit $h_0 \rightarrow -\infty$ and $\gamma \rightarrow 0$ in the above formulas, but we want to quickly discuss it here.

For $\gamma = h = 0$, the Jordan-Wigner transformation maps the Hamiltonian to the tight-binding model

$$H = -\frac{1}{2} \sum_{i=1}^L \hat{c}_i^\dagger \hat{c}_{i+1} + \text{h.c.}, \quad (16)$$

where, \hat{c}_i and \hat{c}_i^\dagger are local spinless fermionic annihilation and creation operators satisfying standard anti-commutation relations. The Hamiltonian (16) can be diagonalised in the momentum basis and can be written as

$$H = \sum_k \epsilon_k \hat{c}_k^\dagger \hat{c}_k, \quad (17)$$

where, $\epsilon_k = -\cos k$ (the velocity is $v(k) = d\epsilon_k/dk = \sin k$ with maximum $v_M = 1$ at $k_M = \pm\pi/2$). \hat{c}_k^\dagger and \hat{c}_k are fermionic creation and annihilation operators in momentum space and they are closely related to the ones in Eq. (10) for the XY chain.

The Néel state in fermionic basis is

$$|\psi_0\rangle = \prod_{i=1}^{L/2} \hat{c}_{2i}^\dagger |0\rangle. \quad (18)$$

It is straightforward to check that for the Néel state in the thermodynamic limit $n_k = 1/2$ for all k , which implies $s(k) = \ln 2$, as it can be also obtained from the limit of Eq. (11). This reflects the fact that all the nonzero overlaps between the Néel state and the eigenstates of the tight-binding chain are equal [151]. The quasiparticle prediction for the entanglement entropy after the Néel quench is obtained by replacing $s(k) = \ln 2$ and $v(k) = v_M \sin k$ in Eq. (4).

B. Numerical study of the entanglement revivals

For free-fermion models the exact dynamics of the entanglement entropy is straightforwardly obtained from the time-dependent fermionic two-point correlations restricted to the subsystem A . This technique is very standard and we do not review it here, the interested reader can consult the extensive literature on the subject [152–154].

Let us first focus on the XX chain (the tight-binding model) after the quench from the Néel state. Our results are reported in Fig. 3. Fig. 3 (a) shows the dynamics of the entanglement entropy S_ℓ for a subsystem of ℓ sites embedded in a chain of size L . We plot the entropy density S_ℓ/ℓ for $\ell = 200$ versus the rescaled time $2v_M t/L$, with v_M the maximum velocity; the entanglement revival time is $t_R = L/(2v_M)$. The dashed lines are the exact numerical results for $L = 600, 800, 1000, 1500$. Several entanglement revivals are visible in the figure. The continuous lines are the predictions using the quasiparticle picture Eq. (3). They are in excellent agreement with the numerical results: in fact $\ell = 200$ is just a finite fraction of the total L considered in the figure and we are safely working in the scaling limit $t, \ell, L \rightarrow \infty$ with fixed ratios.

Now, we study how the height of the dip at the first entanglement revival time is damped as L increases. To quantitatively address this behaviour, we plot δS versus L in Fig. 3 (b). Here δS is defined as in section II, cf. Eq.

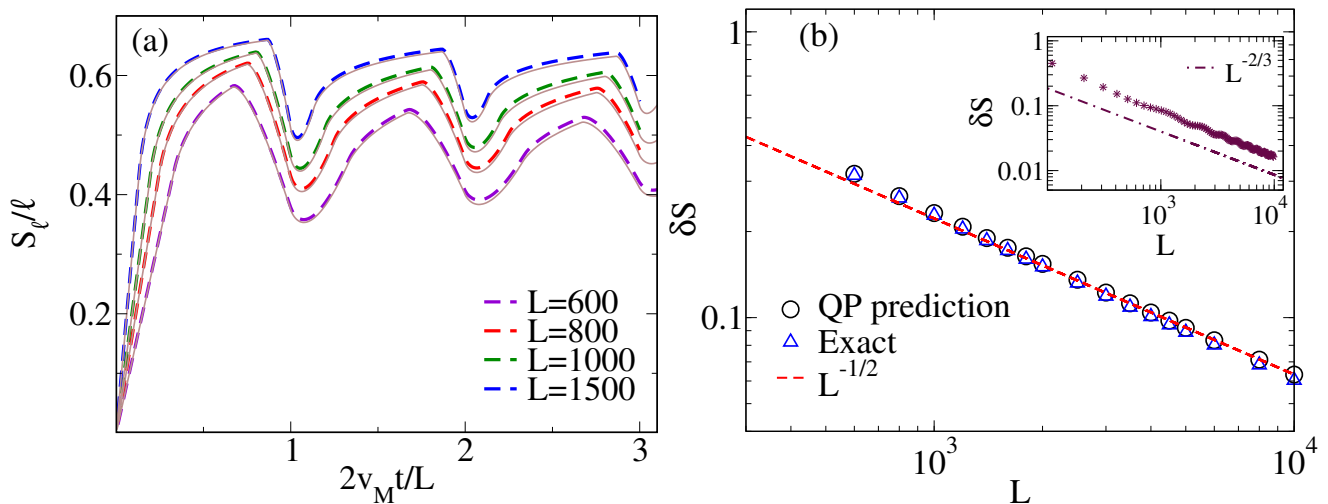


FIG. 3. (a) Entanglement revivals in the XX chain. Quench from the Néel state. S_ℓ/ℓ plotted versus the rescaled time $2v_M t/L$ for $L = 600, 800, 1000, 1500$, and $\ell = 200$. Solid lines correspond to the quasiparticle prediction (see Eq. (4)), while dashed ones are exact numerical data. (b) Scaling of the dip δS of the first entanglement revival. In the main panel, we see that for $\ell = 200$ as L grows from 600 to 10^4 a scaling compatible with the quasiparticle prediction $L^{-1/2}$ is observed neatly. However, for the larger values of L a crossover towards a different scaling starts appearing. This crossover is highlighted in the inset, where we show that for $\ell = 6$ the asymptotic scaling for large L is $\sim L^{-2/3}$ (dot-dashed line).

(5). We show δS as a function of L for fixed $\ell = 200$. It is evident that for the values of L we considered (up to 10^4) the quasiparticle picture works well, since the numerical value for δS and the quasiparticle one stay almost on top of each other. Still, it is evident that as L increases, some deviations between the two appear and a decay faster than $L^{-1/2}$ is starting. To highlight this crossover it is better to use smaller values of ℓ rather than increasing the one of L . Hence, in the inset of 3 (b) we report again the scaling of δS but for $\ell = 6$ rather than 200. In it is clear that in this case the decay of δS with L is much faster and well described by the expected law $L^{-2/3}$. To summarise, Fig. 3 confirms both the quasiparticle decays prediction (8) with $\delta S \sim L^{-1/2}$ at intermediate values of L and the crossover to $L^{-2/3}$ for larger L . We recall that the origin of the exponent $2/3$ is related to the super-diffusion taking place on the light-cone of free fermion models related to Airy processes, see e.g. Refs. [131, 155–160] for similar results. For the quench from the Néel state in the XX chain, the exponent $2/3$ can be derived analytically (see Appendix A).

We end this section by briefly discussing numerical results for the quench in the XY chain. We focus on the Ising case $\gamma = \gamma_0 = 1$. The quench parameters for the transverse fields are fixed as $h = 2, h_0 = 2.4$, but we checked that different values provide equivalent results. Figure 4 summarise our results for fixed $\ell = 100$ and $L = 500, 1000, 2000$. These values have been chosen to be sure to work within the scaling limit with large ℓ, L but with finite ratio. In the main panel we report S_ℓ/ℓ as function of time: the agreement between the numerical data and the quasiparticle prediction is always excellent. Curiously, the first entanglement revival $t_R = L/2v_M$ is quantitatively more pronounced than in the previously considered Néel quench in the XX chain. In the inset of Fig. 4 we fix again $\ell = 100$ and study the scaling of the dip δS as function of L in the window $L \in [500, 6000]$. For these values of L , the numerical data are well captured by the quasiparticle prediction and scaling $\delta S \sim L^{-1/2}$. Also in this case, for the largest considered values of L we observe a crossover towards a faster decay, that once again can be studied in more details. However, we do not perform this investigation here.

IV. FREE BOSONS

In this section we move our attention to a bosonic system, namely the harmonic chain with Hamiltonian

$$H = \frac{1}{2} \sum_{n=0}^{L-1} [\pi_n^2 + m^2 \phi_n^2 + (\phi_{n+1} - \phi_n)^2], \quad (19)$$

with periodic boundary conditions. Eq. (19) defines a chain of L harmonic oscillators with frequency (mass) m and with nearest-neighbor quadratic interactions. Here ϕ_n and π_n are the position and the momentum operators of the n -th oscillator, with equal-time commutation relations $[\phi_m, \pi_n] = i\delta_{nm}$ and $[\phi_n, \phi_m] = [\pi_n, \pi_m] = 0$. Eq. (19) is the lattice discretisation of a one-dimensional Klein-Gordon quantum field theory.

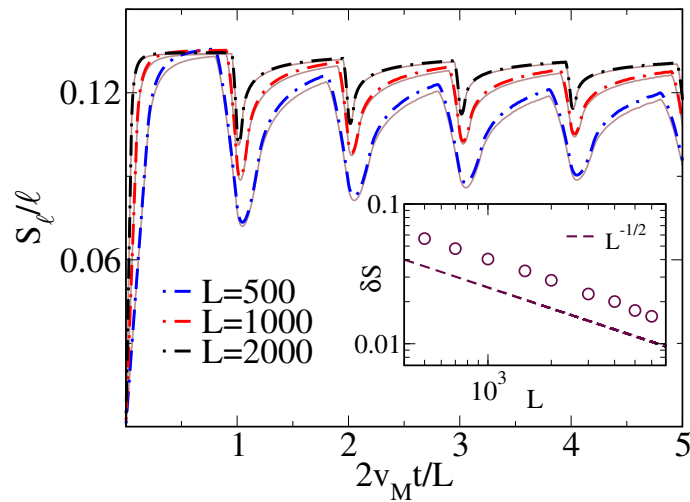


FIG. 4. Entanglement revivals in the XY chain. S_ℓ/ℓ versus rescaled time $2v_M t/L$ for different values of L after the quench from (γ_0, h_0) to (γ, h) , with $\gamma = \gamma_0 = 1$ (Ising model), $h = 2h_0 = 2.4$, and $\ell = 100$. Solid lines correspond to the quasiparticle prediction. The inset shows the scaling of δS with L and the dashed line is a guide to the eye going as $L^{-1/2}$.

The Hamiltonian (19) can be diagonalised in the momentum basis and it can be written as

$$H = \sum_k \epsilon_k \hat{b}_k^\dagger \hat{b}_k, \quad \text{where} \quad \epsilon_k^2 = m^2 + 2(1 - \cos k), \quad (20)$$

and \hat{b}_k^\dagger (\hat{b}_k) is the bosonic creation (annihilation) operator.

Even for the harmonic chain, the GGE density matrix can be constructed from the mode occupation numbers $\hat{n}_k = \hat{b}_k^\dagger \hat{b}_k$ [20, 57], and it is given by

$$\rho_{\text{GGE}} = \frac{e^{-\sum_k \lambda_k \hat{n}_k}}{Z}, \quad (21)$$

where $Z = \text{Tr} e^{-\sum_k \lambda_k \hat{n}_k}$ ensures the normalization $\text{Tr} \rho_{\text{GGE}} = 1$. The Lagrange multipliers λ_k are fixed by imposing that the expectation value of \hat{n}_k in the initial state coincides with its GGE prediction

$$\langle \hat{n}_k \rangle_{\text{GGE}} = -\frac{\partial}{\partial \lambda_k} \sum_p \ln(1 - e^{-\lambda_p}) = \frac{1}{e^{\lambda_k} - 1}. \quad (22)$$

Now λ_k can be obtained by imposing that the expectation value of \hat{n}_k in the initial state $|\psi_0\rangle$ coincides with its GGE prediction, i.e., $\langle \hat{n}_k \rangle_{\text{GGE}} = \langle \psi_0 | \hat{n}_k | \psi_0 \rangle = n_k$. The thermodynamic entropy is

$$S_{\text{GGE}} = -\text{Tr} [\rho_{\text{GGE}} \ln \rho_{\text{GGE}}] = \sum_k (1 + n_k) \ln(1 + n_k) - n_k \ln n_k = \sum_k s(k), \quad (23)$$

where $s(k) = (1 + n_k) \ln(1 + n_k) - n_k \ln n_k$ is identified as the entropy contribution of the quasiparticle with momentum k .

We consider the quantum quench in which the harmonic chain is initially prepared in the ground-state $|\psi_0\rangle$ of the Hamiltonian (19) with $m = m_0$, and at time $t = 0$ the mass is quenched to a different value $m \neq m_0$ [2, 20, 28]. There have been extensive studies focusing on the critical ($m \rightarrow 0$) and continuum limit [36, 37, 103, 142, 161]. The validity of the quasiparticle picture for the entanglement entropy has been tested in all these situations [56, 103, 142, 161]. Note that for the quench to the massless case, a subleading logarithmic correction due to the presence of zero mode appears [161] and for this reason we will stay away from the critical case in the numerical analysis.

We use the notation ϵ_k^0 for the dispersion relation in the initial state and ϵ_k for the one for $t > 0$. The conserved occupation number n_k for this quench is given by [20, 56, 57]

$$n_k = \langle \psi_0 | \hat{n}_k | \psi_0 \rangle = \langle \psi_0 | a_k^\dagger a_k | \psi_0 \rangle = \frac{1}{4} \left(\frac{\epsilon_k}{\epsilon_k^0} + \frac{\epsilon_k^0}{\epsilon_k} \right) - \frac{1}{2}. \quad (24)$$

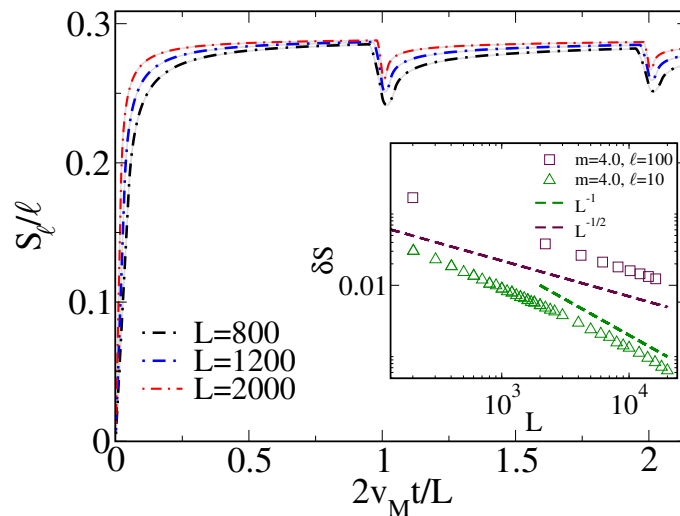


FIG. 5. Entanglement revivals in the harmonic chain. S_ℓ/ℓ versus rescaled time $2v_M t/L$. The data are for the mass quench (from $m_0 = 2$ to $m = 4$), where $\ell = 40$. Solid lines correspond to the quasiparticle prediction and dashed ones to the exact numerical data. The inset shows the height of the entanglement revival δS as a function of L for two different quenches from $m_0 = 2$, both for $\ell = 40$ and $\ell = 10$. While for $\ell = 40$ the power-law $\sim L^{-1/2}$ correctly captures our data, for $\ell = 10$ there is a clear crossover to the truly asymptotic scaling L^{-1} .

We are now ready to study the finite size behaviour of the entanglement entropy after a quench in the harmonic chain. The quasiparticle prediction for the entanglement entropy after this quench is given by Eq. (4) in which we use $s(k)$ given by (23) with (24) and $v(k) = \frac{d\epsilon_k}{dk}$ with ϵ_k in (20). Numerically, the entanglement dynamics is obtained (similarly to the case of free fermions) from the two-point correlation functions by use of standard techniques, as detailed e.g. in Refs. [142, 153, 154, 162]. In Fig. 5 we report the numerical data for the time evolution of the entanglement entropy after the quench of the oscillators' mass from $m_0 = 2$ to $m = 4$ (other values of the masses away from the critical point provide equivalent results), for fixed $\ell = 40$ and $L = 800, 1200, 2000$ chosen to be safely within the scaling limit of large ℓ, L with their ratio finite. The numerical data are compared with the quasiparticle prediction (4) and the agreement is perfect.

We now turn to the study of the dip at the first entanglement revival for the same quench parameters as above. The scaling of δS as obtained from the numerical data is investigated in the inset of Fig. 5 as a function of L (for fixed $\ell = 40$). As expected, since with these parameters we are working in the scaling limit, we perfectly reproduce the scaling $\delta S \propto L^{-1/2}$. However, also for bosons, for larger L we expect a crossover to a different behaviour. Employing the same logic as for fermions, rather than increasing the value of L , it is easier and more effective to reduce the one of ℓ . Hence, in the inset of Fig. 5 we also report the data for $\ell = 10$ that very clearly shows for large L the crossover to the truly asymptotic behaviour L^{-1} . This scaling L^{-1} is just a consequence of the fact that, away from the critical point, the non-equilibrium correlation functions of the harmonic chain are analytic and no singular scaling can take place.

V. THE HEISENBERG XXZ CHAIN AS A PARADIGM OF INTEGRABLE MODEL

To investigate the effect of the interactions, here we consider the paradigm of integrable model, namely the spin-1/2 anisotropic Heisenberg chain (XXZ spin chain). The Hamiltonian is

$$\hat{H} = \sum_{i=1}^{L-1} \left[\frac{1}{2} \left(\hat{S}_i^+ \hat{S}_{i+1}^- + \hat{S}_i^- \hat{S}_{i+1}^+ \right) + \Delta \left(\hat{S}_i^z \hat{S}_{i+1}^z - \frac{1}{4} \right) \right]. \quad (25)$$

Here \hat{S}_i^α are spin-1/2 operators acting at site i of the chain and Δ is the anisotropy parameter. For $\Delta = 0$, it reduces to the XX chain of section III A and it is mapped to free fermions. For $\Delta \neq 0$, the chain is genuinely interacting and it can be solved by the Bethe ansatz [163, 164].

The non-equilibrium dynamics starting from many initial states with low (mainly zero) entanglement has been considered in several manuscripts in the literature [24, 25, 29–31, 165–173], employing different techniques based on integrability. Here, for conciseness, we focus on the non-equilibrium dynamics of the entanglement entropy for a single

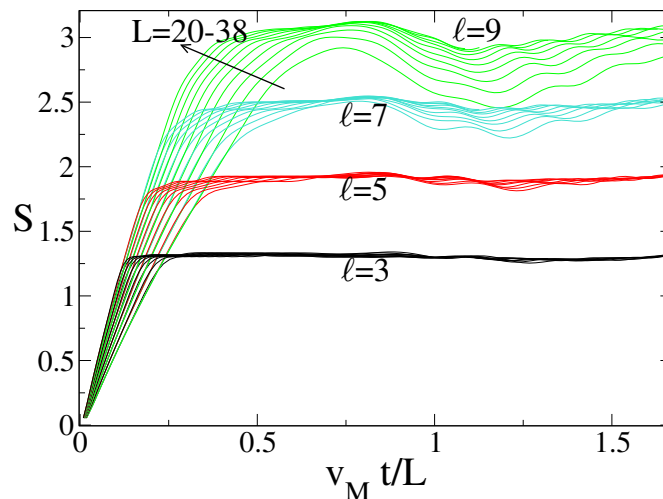


FIG. 6. Time evolution of the entanglement entropy after a quench from the Néel state to the XXZ Hamiltonian with $\Delta = 2$ and with open boundary conditions. Four values of $\ell = 3, 5, 7, 9$ are displayed and L ranges in the interval $L \in [20, 38]$. Revivals are evident for the larger considered ℓ , but their quantitative analysis is made difficult by the presence of spurious finite-size effects. Although we do not report the analysis here, the dip δS at $\ell = 9$ is algebraic with exponent between 1 and 2.

quench, although we expect our results to be more general. Namely, we only consider the dynamics starting from (one of the two degenerate) Néel state

$$|\psi_0\rangle = |\uparrow\downarrow\uparrow\dots\rangle. \quad (26)$$

The GGE describing the steady state after the quench from the Néel state can be constructed analytically using the Quench-Action method [165, 166]. Based on this solution for the Bethe ansatz root density, and exploiting Eq. (3), the quasiparticle prediction for the entanglement dynamics after the quench from the Néel state in the thermodynamic limit has been explicitly written down in Refs. [55, 56] for $\Delta \geq 1$. In Eq. (3) one just needs to interpret $s_n(\lambda)$ as the Yang-Yang entropy densities of the GGE and $v_n(\lambda)$ as the velocities of the excitations built on top of the excited state itself.

However, despite the integrability of the model, calculating the entanglement entropy, even at equilibrium [174], is a daunting task. Furthermore, the study of the time evolution exploiting integrability is extremely difficult even for simpler observables [175, 176]. Hence, in order to access the non-equilibrium dynamics of the entanglement entropy we have to resort to numerical simulations. Here we use tDMRG techniques [177–179]. Consequently, all the data for entanglement dynamics reported in this and in the following Section are obtained using the tDMRG algorithm, as implemented in the iTensor library [180]. We work with the maximum bond dimension $\chi = 2000$ and with a time step $\Delta t = 0.02$ for all simulations. We have checked the robustness of our results by performing simulations for different values of δt and χ . Furthermore, all of our results have been verified with exact diagonalisation for small system sizes.

The only minor drawback of tDMRG is that it works more effectively with open boundary conditions, rather than periodic ones. This is not a main problem for the entanglement revivals dynamics: they are always present in the entanglement dynamics but now they are due to quasiparticles bouncing back at the chain boundaries, rather than going around the full chain. This effect amounts to a minor modification in the semiclassical quasiparticles' trajectories so that the entanglement revival occurs at $t_R = L/v_M$ and not at $t = L/(2v_M)$ as for a periodic chain.

At this point it is rather natural to start our analysis from the case $\Delta \geq 1$ for which an exact solution for the stationary state exists. This implies that we also know exactly the value of the maximal velocity and the stationary entropy, both important for the study of the dip of the entanglement revivals. The numerical time evolution of the entanglement entropy after a quench from the Néel state to the XXZ Hamiltonian is reported in Fig. 6 for $\Delta = 2$ (different values for all $\Delta \geq 1$ produces qualitatively equivalent results). With tDMRG we can access relatively small values of ℓ and L . In the figure we report $\ell = 3, 5, 7, 9$ (the data for even ℓ would be too close and make the figure difficult to read, but they are very similar) and we focus on L in the interval $L \in [20, 38]$. With a large numerical effort it is possible to increase slightly these values, but for a more quantitative analysis, one needs to at least double both ℓ and L . In the figure, entanglement revivals are evident for $\ell = 7$ and $\ell = 9$, although they take place slightly after L/v_M . This is clearly due to the presence of many species of particles (called strings) which are not yet well separated for $\ell = 9$. The resulting finite size effects are huge and a quantitative analysis of the dip of the entanglement revival

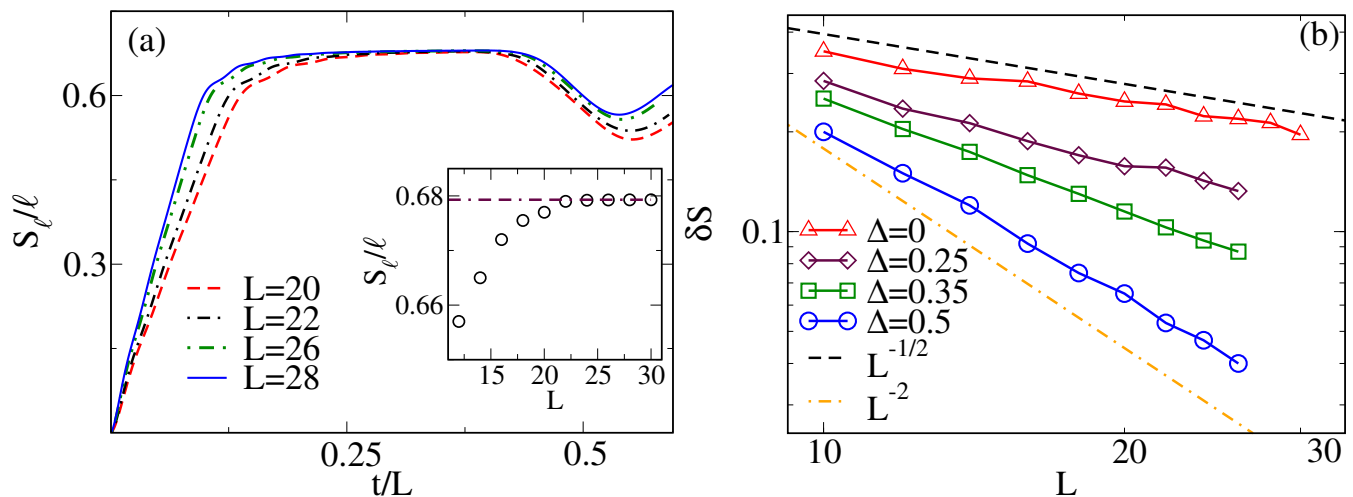


FIG. 7. Entanglement revivals in the Heisenberg chain for $\Delta < 1$ with tDMRG simulations for open boundary conditions. (a) S_ℓ/ℓ versus rescaled time t/L for $\Delta = 0.25$. Several values of L are shown. The value of ℓ is fixed to $\ell = 4$. The inset shows the density of entanglement entropy S_ℓ/ℓ in the plateau as a function of L . The dashed line is the extracted value for the steady state entropy. (b) The scaling of the dip δS as a function of L for $\Delta = 0, 0.25, 0.35, 0.5$. The dashed (dot-dashed) line is a guide to the eye going like $\sim L^{-1/2}$ (L^{-2}).

is unstable, although we know a priori the values of t_R and $S_\ell(\infty)$ that enter in the definition (5) of δS . Although we do not present any analysis of the dip of the first entanglement revival, the data at both $\ell = 9$ and $\ell = 7$ are well compatible with an algebraic decay of δS with an exponent which is between 1 and 2. This is different from the quasiparticle prediction $1/2$, but we cannot conclude whether this is due to the oscillations of the data or to the fact that we are not yet in the scaling regime, although we tend to believe more to the second explanation.

Since the data for $\Delta > 1$ are quantitatively not convincing enough, it is rather natural to move our attention to the window $\Delta \in [0, 1)$. The main advantage is that we expect smaller finite size effects because (at rational values of Δ) the number of species of quasiparticles is finite (often small) and so they should produce less interference effects and clearer entanglement revivals. The steady-state after the quench from the Néel state can be in principle obtained by using the approach of Ref. 31 (see also 24 and 181). Hence, we do not know exactly either the value of $S_\ell(\infty)$ or that of t_R (because we do not know v_M). The time evolution of the entanglement entropy for $\Delta = 0.25$ is reported in Figure 7(a). We focus on $\ell = 4$ and L in the range $L \in [20, 28]$. The reason of this small value of ℓ (compared to the study at $\Delta > 1$ in Fig. 6) is that the entanglement entropy grows much faster (its asymptotic density is more than the double than at $\Delta = 2$), limiting the performance of the tDMRG algorithm. However, even at this small value of ℓ we see a neat first entanglement revival with very small finite size effects, confirming our expectations. In this case, we do not know the asymptotic value of the entropy, but we can extract it in a very robust manner from the numerics since the plateau is very stable (as a difference with the case $\Delta > 1$). The determination $S_4(\infty)$ is reported for $\Delta = 0.25$ in the inset of Fig. 7(a). Curiously enough, the asymptotic value $S_\ell(\infty)$ depends very little on Δ in all the window $\Delta \in [0, 1)$ and it is very close to the value at $\Delta = 0$, i.e. $\ell \ln 2$ (but it is definitively different). In order to study the behaviour of the dip of δS as function of L (see again Fig. 1 (a)) for fixed ℓ , we would need to know v_M to extract t_R . To circumvent this problem, we instead use in Eq. (5) the very neat minimum that the entanglement entropy displays. The difference between $S_\ell(t_R)$ and the minimum is anyhow expected to shrink and go to zero for large L ; so, in the worst case scenario, this replacement introduces just a further finite size effect. Calculating δS in this way, we report our data for several $\Delta \in [0, 1]$ in Fig. 7 (b), all for $\ell = 4$. Since the plot is in log-log scale, the data are all fully compatible with a power-law behaviour with an exponent between $1/2$ and 2 (these two extremes are shown as guides to the eyes in the plots). We could also extract effective exponents for the decay, but we do not find their values significative for these small value of ℓ and L .

We stress that upon increasing the values of ℓ and L , we expect the data to crossover to the quasiparticle picture results with a behaviour of the dip going like $L^{-1/2}$, also in the presence of interactions for any Δ . However, unlike for free models, here we are restricted to the system size $L \simeq 30 - 40$ due to the limitation of available numerical techniques. Hence, the quasiparticle regime cannot be accessed. In fact, the prediction for the time evolution from the quasiparticle picture in Fig. 6 together with the numerical data for $\Delta > 1$, the agreement would be satisfactory only at short time, as already shown in Refs. [55, 56]. Anyhow, in spite of the many drawbacks of this quantitative analysis, we can conclude, without doubts, that the decay of the dip of the entanglement revival is algebraic with an

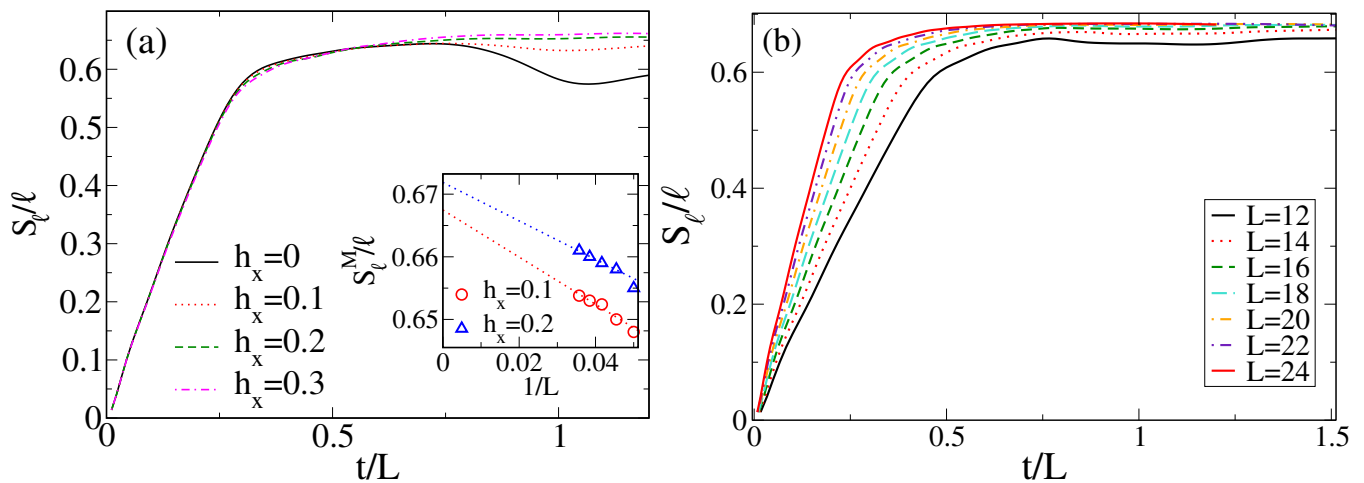


FIG. 8. Entanglement revivals in the non-integrable Heisenberg chain (27) with open boundary conditions after a quench from the Néel state. (a) Entropy density S_ℓ/ℓ for $L = 18$ and $\ell = 4$ versus rescaled time t/L . Here $\Delta = 0.5$ and $h_x = 0, 0.1, 0.2, 0.3$. The inset shows the maximum of S_ℓ/ℓ versus L for $h_x = 0.1, 0.2$. Dashed lines corresponds to the best fit to $S_\ell^M/\ell = S_\ell(\infty)/\ell + a/L$ with $S_\ell(\infty)$ and a fitting parameters. (b) The same as in (a) but at fixed $h_x = 0.2$ with varying L .

exponent between $1/2$ and 2 for all values of Δ . Such a conclusion also reinforces the same result found for $\Delta > 1$ but with less stable data.

VI. INTERACTIONS THAT BREAK INTEGRABILITY

We have verified in the previous sections the validity of the quasiparticle picture Eq. (4) to describe the entanglement revivals in free fermionic and free bosonic models. Moreover, we showed that the dip in the entanglement entropy at the entanglement revival time is damped as $L^{-1/2}$ in the scaling regime (cf. (8)) for free-fermion and free-boson models. For interacting integrable models it is difficult to access the scaling regime, but we can anyhow show that the decays of the dip is algebraic with L . We now discuss the effects of integrability breaking.

As an example of a chaotic model, we consider a non-integrable perturbation added to the XXZ Hamiltonian (25), in such a way to have an integrable limit. Among the various possibilities to break integrability, we opt for the addition of a longitudinal magnetic field h_x modifying the Hamiltonian as

$$\hat{H} = \sum_{i=1}^{L-1} \frac{1}{2} \left(\hat{S}_i^+ \hat{S}_{i+1}^- + \hat{S}_i^- \hat{S}_{i+1}^+ \right) + \Delta \left(\hat{S}_i^z \hat{S}_{i+1}^z - \frac{1}{4} \right) + h_x \sum_i \hat{S}_i^x. \quad (27)$$

The Hamiltonian (25) is non-integrable except at the isotropic point $\Delta = 1$.

As for the integrable XXZ chain, we use tDMRG simulation to access the entanglement dynamics following a quench governed by the Hamiltonian (27). Again we focus on the dynamics starting from the Néel state and we only consider $\Delta = 0.5$ which is far enough from the integrable point at $\Delta = 1$. Figure 8 shows the entanglement evolution for different values of h_x for fixed $\ell = 4$ and various L (only (b) panel). It is clear from Fig. 8(a) that, at fixed L , the entanglement revival fades away as the integrability breaking parameter h_x is increased. However, to perform a quantitative analysis of the dip δS , we need first to numerically extract $S_\ell(\infty)$. Unlike the integrable case (see Fig. 7), here we observe clear finite-size effects. In the inset of Fig. 8(a), we show the maximum of S_ℓ/ℓ as a function of $1/L$. The data suggest to fit S_ℓ^M/ℓ with a linear form $S_\ell^M/\ell = S_\ell(\infty)/\ell + a/L$ (where $S_\ell(\infty)$ and a are fitting parameters). Interestingly, we observe that $S_\ell(\infty)/\ell \approx 0.67$, which is close to the maximum entropy density $\ln 2$, which is also the value at $\Delta = h_x = 0$. Since the model is not integrable, t_R is not well defined, so in the definition of δS we can use the minimum of S_ℓ close to the entanglement revival, as we did for the integrable XXZ spin-chain. Anyhow it is very difficult to evaluate this minimum for $h_x \neq 0$ as soon as L is moderately large. For example in Fig. 8 (b) we report the time evolution of the entanglement entropy at fixed $h_x = 0.2$, but for different values of L . We can observe a small entanglement revival only for $L = 12$, but for larger L the decay is too fast to identify a clear minimum in the entropy. If one attempts an analysis at this not well-identified dip, the decay is much faster than any power-law, likely exponential, but could be even faster. Our findings match well the results found in Ref. [80] from the scaling of the peak of the mutual information. This is not surprising because the physical origin of the mutual information

scrambling and of the decay of the entanglement revivals is the same, i.e. that in non-integrable systems there are no well defined quasiparticles which can preserve quantum correlations over large distance and long times. We should mention that the random unitary [120] framework predicts the absence of revival, as it is observed in Ref. 74.

VII. CONCLUSIONS

In this work we investigated the revivals of the entanglement entropy of an interval of fixed length after a quantum quench in finite-size systems. Our main result is that both in integrable and in non-integrable systems the strength of the entanglement revival is damped as a function of the system size. However, while the damping is algebraic for integrable systems, it is much faster in chaotic ones (strong scrambling). Within the quasiparticle picture for the entanglement spreading of integrable models, the exponent of the power-law decay is $1/2$. However, we provide compelling evidence that this exponent describes only an intermediate regime for $\ell = aL$ with $a \ll 1$. For very small ℓ , there is a crossover toward a truly asymptotic regime with a model dependent exponent which is larger than $1/2$ (e.g., it is equal to $2/3$ for the XX chain and to 1 for gapped free bosons). Our results suggest that the entanglement revivals provide a useful tool to diagnose scrambling in quantum many-body systems.

There are several interesting directions for future work. A simple generalisation of our work would be to understand the scaling of entanglement revivals in higher-dimensional free models, for which the same techniques used here trivially apply. A more difficult generalisation would be to understand what happens for Rényi entropies. Indeed, while for integrable models the quasiparticle picture is expected to work (with some troubles though, see Refs. [138–141]), for chaotic systems with a conserved charge there are effects of diffusion also at intermediate times [182–185] and it is unclear how they could affect the entanglement revivals. Another natural question concerns whether entanglement revivals can survive to the addition of some quenched disorder and, if yes, how they disappear as the system size grows. Finally, in this work we focused on entanglement revivals after a global quantum quench. However, entanglement revivals are expected also in different non-equilibrium protocols such as, just to quote two examples, the domain-wall quench [186–188] and geometric quenches [189, 190]. It would be interesting to understand the damping of entanglement revivals also in these situations.

Finally, it has been suggested recently that the eigenstate-average of the entanglement entropy can potentially distinguish between integrable and chaotic systems [191]. Specifically, the prefactor of the volume-law entropy seems to exhibit a marked difference between integrable and chaotic dynamics, and it depends in a nontrivial fashion on the aspect ratio ℓ/L . It would be interesting to devise an out-of-equilibrium protocol that allows to reveal this behavior, for instance considering Floquet systems. This could provide a further out-of-equilibrium diagnostic tool to distinguish integrable versus chaotic models.

VIII. ACKNOWLEDGMENTS

VA acknowledges support from the European Research Council under ERC Advanced grant 743032 DYNAMINT. PC acknowledges support from ERC under Consolidator grant number 771536 (NEMO).

Appendix A: Decay of entanglement revival in the XX chain after the Néel quench

Here we derive the exponent $2/3$ of the decay of the entanglement revival after the quench from the Néel state in the XX chain (see section III B).

A straightforward application of Wick's theorem gives the correlation matrix $C_{nm} \equiv \langle \text{Neel} | c^\dagger(t)c(t) | \text{Neel} \rangle$ after the Néel quench as

$$C_{nm} = \frac{1}{2}\delta_{nm} + \frac{(-1)^m}{2} \frac{1}{L} \sum_{k=-(L-1)/2}^{(L-1)/2} e^{-i2\pi k/L(n-m)+2it \cos(2\pi k/L)} \quad (\text{A1})$$

One has to derive the asymptotic behavior of C_{nm} in the limit $L \rightarrow \infty$. This can be done in a standard way by using the Poisson summation formula. For a generic periodic function $G(x) = G(x + 2\pi)$ this states that

$$\frac{1}{L} \sum_{k=-(L-1)/2}^{(L-1)/2} G(2\pi k/L) = \frac{1}{2\pi} \sum_{l=-\infty}^{\infty} \int_{-\pi}^{\pi} dq G(q) e^{iqL}. \quad (\text{A2})$$

Now, Eq. (A1) gives

$$C_{nm} = \frac{1}{2}\delta_{nm} + \frac{(-1)^m}{2} \frac{1}{2\pi} \sum_{l=-\infty}^{\infty} \int_{-\pi}^{\pi} dq e^{-iq(lL-n+m)+2it \cos q} \quad (\text{A3})$$

The integral above can be performed analytically to obtain

$$C_{nm} = \frac{1}{2}\delta_{nm} + \frac{(-1)^m}{2} \sum_{l=-\infty}^{\infty} i^{lL-n+m} J_{lL-n+m}(2t), \quad (\text{A4})$$

where $J_p(x)$ is the Bessel function of the first kind.

To proceed we consider the correlation function at the revival time $t = L/2$. Thus, a straightforward analysis of the asymptotic behavior of the Bessel functions in the limit $L \rightarrow \infty$, or, equivalently a saddle point treatment of the integral in (A3) shows that the terms with $l \neq -1, 0, 1$ give exponentially suppressed contributions in the limit $L \rightarrow \infty$. The remaining terms give

$$C_{nm} = \frac{1}{2}\delta_{nm} + \frac{6^{\frac{1}{3}}(-1)^{m+1} \cos\left(\frac{1}{2}\pi(n-m)\right)}{L^{\frac{1}{3}}\Gamma\left(-\frac{1}{3}\right)} + \frac{i^{n+m} \sin\left(\frac{1}{4}(4L-2\pi n+2\pi m+\pi)\right)}{\sqrt{2\pi}\sqrt{L}}, \quad (\text{A5})$$

where $\Gamma(x)$ is the Euler Gamma function. It is important to observe that the first term in (A5) exhibits the decay as $1/L^{1/3}$, whereas the second one is $\propto 1/L^{1/2}$. The first term originates from the fact that for $l = \pm 1$ the saddle point contribution in the integral in (A3) vanishes. The second one is the saddle point contribution for $l = 0$. By using (A5) it is now straightforward to derive the behavior of entanglement entropy of a finite subsystem in the limit $L \rightarrow \infty$. As for the mutual information [80], to understand the behavior of the entanglement entropy at the revival time in the large L limit, one can consider a subsystem of length $\ell = 2$. An explicit calculation shows that δS (cf. 1 (a)) decays as $1/L^{2/3}$. It is important to observe that the exponent $1/3$ is the same arising in the description of super-diffusion on the light-cone in free fermion models. This is not surprising because the derivation outlined above is the same.

-
- [1] G. Mussardo, Statistical field theory: an introduction to exactly solved models in statistical physics, **2nd edition**, Oxford University Press (2020).
 - [2] P. Calabrese and J. Cardy, Time-dependence of correlation functions following a quantum quench, **Phys. Rev. Lett.** **96** 136801 (2006).
 - [3] P. Calabrese, F. H. L. Essler, and G. Mussardo, Introduction to ‘‘Quantum Integrability in Out of Equilibrium Systems’’, **J. Stat. Mech.** (2016) P064001.
 - [4] J. von Neumann, Beweis des Ergodensatzes und des H-Theorems, **Z Phys.** **57**, 30 (1929).
 - [5] R. V. Jensen and R. Shankar, Statistical behaviour in Deterministic Quantum Systems with Few Degrees of Freedom, **Phys. Rev. Lett.** **54**, 1879 (1985).
 - [6] J. M. Deutsch, Quantum statistical mechanics in a closed system, **Phys. Rev. A** **43**, 2046 (1991).
 - [7] M. Srednicki, Chaos and quantum thermalisation, **Phys. Rev. E** **50**, 888 (1994).
 - [8] M. Rigol, V. Dunjko, and M. Olshanii, Thermalisation and its mechanism for generic isolated quantum systems, **Nature** **452**, 854 (2008).
 - [9] M. Rigol and M. Srednicki, Alternatives to Eigenstate thermalisation, **Phys. Rev. Lett.** **108**, 110601 (2012).
 - [10] L. D’Alessio, Y. Kafri, A. Polkovnikov, and M. Rigol, From Quantum Chaos and Eigenstate thermalisation to Statistical Mechanics and Thermodynamics, **Adv. Phys.** **65**, 239 (2016).
 - [11] C. Gogolin and J. Eisert, Equilibration, thermalisation, and the emergence of statistical mechanics in closed quantum systems, **Rep. Prog. Phys.** **79**, 056001 (2016).
 - [12] M. Rigol, V. Dunjko, V. Yurovsky, and M. Olshanii, Relaxation in a Completely Integrable Many-Body Quantum System: An *Ab Initio* Study of the Dynamics of the Highly Excited States of 1D Lattice Hard-Core Bosons. **Phys. Rev. Lett.** **98**, 050405 (2007).
 - [13] M. A. Cazalilla, Effect of Suddenly Turning on Interactions in the Luttinger Model, **Phys. Rev. Lett.** **97**, 156403 (2006).
 - [14] T. Barthel and U. Schollwöck, Dephasing and the Steady State in Quantum Many-Particle Systems. **Phys. Rev. Lett.** **100**, 100601 (2008).
 - [15] M. Cramer, C. M. Dawson, J. Eisert, and T. J. Osborne, Exact Relaxation in a Class of Nonequilibrium Quantum Lattice Systems, **Phys. Rev. Lett.** **100**, 030602 (2008).
 - [16] M. Cramer and J. Eisert, A quantum central limit theorem for non-equilibrium systems: exact local relaxation of correlated states, **New J. Phys.** **12**, 055020 (2010).
 - [17] S. Sotiriadis, P. Calabrese, and J. Cardy, Quantum Quench from a Thermal Initial State, **EPL** **87**, 20002 (2009).

- [18] M. A. Cazalilla, A. Iucci, and M.-C. Chung, Thermalisation and quantum correlations in exactly solvable models, *Phys. Rev. E* **85**, 011133 (2012).
- [19] P. Calabrese, F. H. L. Essler, and M. Fagotti, Quantum Quench in the Transverse-Field Ising Chain, *Phys. Rev. Lett.* **106**, 227203 (2011);
P. Calabrese, F. H. L. Essler, and M. Fagotti, Quantum quench in the transverse field Ising chain: I. Time evolution of order parameter correlators, *J. Stat. Mech.* (2012) P07016;
P. Calabrese, F. H. L. Essler, and M. Fagotti, Quantum quenches in the transverse field Ising chain: II. Stationary state properties, *J. Stat. Mech.* (2012) P07022.
- [20] P. Calabrese and J. Cardy, Quantum quenches in extended systems, *J. Stat. Mech.* (2007) P06008.
- [21] J. Mossel and J.-S. Caux, Generalized TBA and generalized Gibbs, *J. Phys. A* **45**, 255001 (2012).
- [22] D. Fioretto and G. Mussardo, Quantum quenches in integrable field theories, *New J. Phys.* **12**, 055015 (2010);
S. Sotiriadis, D. Fioretto, and G. Mussardo, Zamolodchikov-Faddeev algebra and quantum quenches in integrable field theories, *J. Stat. Mech.* (2012) P02017.
- [23] M. Collura, S. Sotiriadis, and P. Calabrese, Equilibration of a Tonks-Girardeau Gas Following a Trap Release, *Phys. Rev. Lett.* **110**, 245301 (2013);
M. Collura, S. Sotiriadis, and P. Calabrese, Quench dynamics of a Tonks-Girardeau gas released from a harmonic trap, *J. Stat. Mech.* (2013) P09025.
- [24] M. Fagotti and F. H. L. Essler, Stationary behaviour of observables after a quantum quench in the spin-1/2 Heisenberg XXZ chain, *J. Stat. Mech.* (2013) P07012.
- [25] B. Pozsgay, The generalized Gibbs ensemble for Heisenberg spin chains, *J. Stat. Mech.* P07003 (2013).
- [26] M. Fagotti and F. H. L. Essler, Reduced Density Matrix after a Quantum Quench, *Phys. Rev. B* **87**, 245107 (2013).
- [27] M. Fagotti, Finite-size corrections vs. relaxation after a sudden quench, *Phys. Rev. B* **87**, 165106 (2013).
- [28] S. Sotiriadis and P. Calabrese, Validity of the GGE for quantum quenches from interacting to noninteracting models, *J. Stat. Mech.* (2014) P07024.
- [29] M. Fagotti, M. Collura, F. H. L. Essler, and P. Calabrese, Relaxation after quantum quenches in the spin-1/2 Heisenberg XXZ chain, *Phys. Rev. B* **89**, 125101 (2014).
- [30] E. Ilievski, J. De Nardis, B. Wouters, J.-S. Caux, F. H. L. Essler, and T. Prosen, Complete Generalized Gibbs Ensembles in an Interacting Theory, *Phys. Rev. Lett.* **115**, 157201 (2015).
- [31] E. Ilievski, E. Quinn, J. D. Nardis, and M. Brockmann, String-charge duality in integrable lattice models, *J. Stat. Mech.* (2016) 063101.
- [32] V. Alba, Simulating the Generalized Gibbs Ensemble (GGE): a Hilbert space Monte Carlo approach. [arXiv:1507.06994](https://arxiv.org/abs/1507.06994).
- [33] T. Langen, S. Erne, R. Geiger, B. Rauer, T. Schweigler, M. Kuhnert, W. Rohringer, I. E. Mazets, T. Gasenzer, and J. Schmiedmayer, Experimental observation of a generalized Gibbs ensemble, *Science* **348**, 207 (2015).
- [34] F. H. L. Essler, G. Mussardo, and M. Panfil, Generalized Gibbs ensembles for quantum field theories, *Phys. Rev. A* **91**, 051602 (2015);
F. H. L. Essler, G. Mussardo, and M. Panfil, On Truncated Generalized Gibbs Ensembles in the Ising Field Theory, *J. Stat. Mech.* (2017) 013103.
- [35] J. Cardy, Quantum quenches to a critical point in one dimension: some further results, *J. Stat. Mech.* (2016) 023103.
- [36] S. Sotiriadis, Memory-preserving equilibration after a quantum quench in a 1d critical model, *Phys. Rev. A* **94**, 031605 (2016).
- [37] A. Bastianello and S. Sotiriadis, Quasi locality of the GGE in interacting-to-free quenches in relativistic field theories, *J. Stat. Mech.* (2017) 023105.
- [38] E. Vernier and A. Cortés Cubero, Quasilocal charges and the complete GGE for field theories with non diagonal scattering, *J. Stat. Mech.* (2017) 23101.
- [39] B. Pozsgay, E. Vernier, and M. A. Werner, On Generalized Gibbs Ensembles with an infinite set of conserved charges, *J. Stat. Mech.* (2017) 093103.
- [40] L. Vidmar and M. Rigol, Generalized Gibbs ensemble in integrable lattice models, *J. Stat. Mech.* (2016) 064007.
- [41] F. H. L. Essler and M. Fagotti, Quench dynamics and relaxation in isolated integrable quantum spin chains, *J. Stat. Mech.* (2016) 064002.
- [42] L. Foini, A. Gambassi, R. Konik, and L. F. Cugliandolo, Measuring effective temperatures in a generalized Gibbs ensemble, *Phys. Rev. E* **95**, 052116 (2017).
- [43] T. Palmai and R. M. Konik, Quasi-local charges and the Generalized Gibbs Ensemble in the Lieb-Liniger model, *Phys. Rev. E* **98**, 052126 (2018).
- [44] E. Ilievski, M. Mednjak, T. Prosen, and L. Zadnik, Quasilocal charges in integrable lattice systems, *J. Stat. Mech.* (2016) P064008.
- [45] T. Langen, T. Gasenzer, and J. Schmiedmayer, Prethermalisation and universal dynamics in near-integrable quantum systems, *J. Stat. Mech.* (2016) 064009.
- [46] M. Marcuzzi, J. Marino, A. Gambassi, and A. Silva, Prethermalization in a Nonintegrable Quantum Spin Chain after a Quench, *Phys. Rev. Lett.* **111**, 197203 (2013).
- [47] F. H. L. Essler, S. Kehrein, S. R. Manmana, and N. J. Robinson, Quench dynamics in a model with tuneable integrability breaking, *Phys. Rev. B* **89**, 165104 (2014).
- [48] G. P. Brandino, J.-S. Caux, and R. M. Konik, Glimmers of a Quantum KAM Theorem: Insights from Quantum Quenches in One-Dimensional Bose Gases, *Phys. Rev. X* **5**, 041043 (2015).
- [49] B. Bertini and M. Fagotti, Pre-relaxation in weakly interacting models, *J. Stat. Mech.* (2015) P07012.

- [50] B. Bertini, F. H. L. Essler, S. Groha, and N. J. Robinson, Prethermalization and Thermalization in Models with Weak Integrability Breaking, *Phys. Rev. Lett.* **115**, 180601 (2015).
- [51] M. Fagotti and M. Collura, Universal prethermalization dynamics of entanglement entropies after a global quench, [arXiv:1507.02678](https://arxiv.org/abs/1507.02678) (2015).
- [52] M. Marcuzzi, J. Marino, A. Gambassi, and A. Silva, Prethermalization from a low-density Holstein-Primakoff expansion, *Phys. Rev. B* **94**, 214304 (2016).
- [53] V. Alba and M. Fagotti, Prethermalization at low temperature: the scent of a spontaneously broken symmetry, *Phys. Rev. Lett.* **119**, 010601 (2017).
- [54] P. Calabrese and J. Cardy, Evolution of Entanglement Entropy in One-Dimensional Systems, *J. Stat. Mech.* (2005) P04010.
- [55] V. Alba and P. Calabrese, Entanglement and thermodynamics after a quantum quench in integrable systems, *PNAS* **114**, 7947 (2017).
- [56] V. Alba and P. Calabrese, Entanglement dynamics after quantum quenches in generic integrable systems, *SciPost Phys.* **4**, 017 (2018).
- [57] P. Calabrese, Entanglement and thermodynamics in non-equilibrium isolated quantum systems, *Physica A* **504**, 31 (2018).
- [58] P. Zanardi, Entanglement of quantum evolutions, *Phys. Rev. A* **63**, 040304 (2001).
- [59] T. Prosen and I. Pizorn, Operator space entanglement entropy in a transverse Ising chain, *Phys. Rev. A* **76**, 032316 (2007).
- [60] T. Prosen and M. Znidaric, Is the efficiency of classical simulations of quantum dynamics related to integrability?, *Phys. Rev. E* **75**, 015202(R) (2007).
- [61] M. Znidaric, T. Prosen, and I. Pizorn, Complexity of thermal states in quantum spin chains, *Phys. Rev. A* **78**, 022103 (2008).
- [62] I. Pizorn and T. Prosen, Operator Space Entanglement Entropy in XY Spin Chains, *Phys. Rev. B* **79**, 184416 (2009).
- [63] J. Dubail, Entanglement scaling of operators: a conformal field theory approach, with a glimpse of simulability of long-time dynamics in 1+1 d, *J. Phys. A* **50**, 234001 (2017).
- [64] J. Maldacena, S. H. Shenker, and D. Stanford, A bound on chaos, *JHEP* **08** (2016) 106.
- [65] M. Blake, H. Lee, and H. Liu, A quantum hydrodynamical description for scrambling and many-body chaos, *JHEP* **10** (2018) 127.
- [66] V. Khemani, D. A. Huse, and A. Nahum, Velocity-dependent Lyapunov exponents in many-body quantum, semiclassical, and classical chaos, *Phys. Rev. B* **98**, 144304 (2018).
- [67] S. Gopalakrishnan, D. A. Huse, V. Khemani, and R. Vasseur, Hydrodynamics of operator spreading and quasiparticle diffusion in interacting integrable systems, *Phys. Rev. B* **98**, 220303(R) (2018).
- [68] P. Hayden and J. Preskill, Black holes as mirrors: quantum information in random subsystems, *JHEP* **09** (2007) 120.
- [69] Y. Sekino and L. Susskind, Fast Scramblers, *JHEP* **10** (2008) 065.
- [70] S. H. Shenker and D. Stanford, Black holes and the butterfly effect, *JHEP* **03** (2014) 067.
- [71] P. Hosur, X.-L. Qi, D. A. Roberts, and B. Yoshida, Chaos in quantum channels, *JHEP* **02** (2016) 004.
- [72] S. Pappalardi, A. Russomanno, B. Zunkovic, F. Iemini, A. Silva, and R. Fazio, Scrambling and entanglement spreading in long-range spin chains, *Phys. Rev. B* **98**, 134303 (2018).
- [73] V. Alba, J. Dubail, and M. Medenjak Operator Entanglement in Interacting Integrable Quantum Systems: the Case of the Rule 54 Chain, *Phys. Rev. Lett.* **122**, 250603 (2019).
- [74] B. Bertini, P. Kos, and T. Prosen, Operator Entanglement in Local Quantum Circuits I: Chaotic Dual-Unitary Circuits, [arXiv:1909.07407](https://arxiv.org/abs/1909.07407);
B. Bertini, P. Kos, and T. Prosen, Operator Entanglement in Local Quantum Circuits II: Solitons in Chains of Qubits, [arXiv:1909.07410](https://arxiv.org/abs/1909.07410).
- [75] L. Nie, M. Nozaki, S. Ryu, and M. T. Tan, Signature of quantum chaos in operator entanglement in 2d CFTs, *J. Stat. Mech.* (2019) 093107.
- [76] C. T. Asplund and A. Bernamonti, Mutual information after a local quench in conformal field theory, *Phys. Rev. D* **89**, 066015 (2014).
- [77] V. Balasubramanian, A. Bernamonti, N. Copland, B. Craps, and F. Galli, Thermalization of mutual and tripartite information in strongly coupled two dimensional conformal field theories, *Phys. Rev. D* **84**, 105017 (2011).
- [78] C. T. Asplund, A. Bernamonti, F. Galli, and T. Hartmann, Entanglement scrambling in 2D conformal field theory, *JHEP* **09** (2015) 110.
- [79] S. Leichenauer and M. Moosa, Entanglement tsunami in (1+1)-dimensions, *Phys. Rev. D* **92**, 126004 (2015).
- [80] V. Alba and P. Calabrese, Quantum information scrambling after a quantum quench, *Phys. Rev. B* **100**, 115150 (2019).
- [81] R. Vasseur, S. A. Parameswaran, and J. E. Moore, Quantum revivals and many-body localization, *Phys. Rev. B* **91**, 140202 (2015).
- [82] A. A. Michailidis, C. J. Turner, Z. Papic, D. A. Abanin, and M. Serbyn, Slow Quantum Thermalization and Many-Body Revivals from Mixed Phase Space *Phys. Rev. X* **10**, 011055 (2020).
- [83] J. Cardy, Thermalization and Revivals after a Quantum Quench in Conformal Field Theory, *Phys. Rev. Lett.* **112**, 220401 (2014).
- [84] J.M. Stéphan and J. Dubail, Local quantum quenches in critical one-dimensional systems: entanglement, the Loschmidt echo, and light-cone effects, *J. Stat. Mech.* (2011), 08019.
- [85] K. Najafi and M. A. Rajabpour, On the possibility of complete revivals after quantum quenches to a critical point, *Phys. Rev. B* **96**, 014305 (2017).

- [86] K. Najafi, M. A. Rajabpour, and J. Viti, Return amplitude after a quantum quench in the XY chain, *J. Stat. Mech.* **(2019)** 083102.
- [87] K. Najafi, M. A. Rajabpour, and J. Viti, Light-cone velocities after a global quench in a noninteracting model, *Phys. Rev. B* **97**, 205103 (2018)
- [88] B. Bertini, P. Kos, and T. Prosen, Entanglement spreading in a minimal model of maximal many-body quantum chaos, *Phys. Rev. X* **9**, 021033 (2019).
- [89] L. Piroli, B. Bertini, J. I. Cirac, and T. Prosen, Exact dynamics in dual-unitary quantum circuits, *Phys. Rev. B* **101**, 094304 (2020).
- [90] A. Chan, A. De Luca, J. T. Chalker, Solution of a minimal model for many-body quantum chaos, *Phys. Rev. X* **8**, 041019 (2018).
- [91] R. Islam, R. Ma, P. M. Preiss, M. E. Tai, A. Lukin, M. Rispoli, and M. Greiner, Measuring entanglement entropy in a quantum many-body system, *Nature* **528**, 77 (2015).
- [92] A. M. Kaufman, M. E. Tai, A. Lukin, M. Rispoli, R. Schittko, P. M. Preiss, and M. Greiner, Quantum thermalisation through entanglement in an isolated many-body system, *Science* **353**, 794 (2016).
- [93] A. Daley, H. Pichler, J. Schachenmayer, and P. Zoller, Measuring entanglement growth in quench dynamics of bosons in an optical lattice, *Phys. Rev. Lett.* **109**, 020505 (2012).
- [94] A. Elben, B. Vermersch, M. Dalmonte, J. I. Cirac and P. Zoller, Rényi Entropies from Random Quenches in Atomic Hubbard and Spin Models, *Phys. Rev. Lett.* **120**, 050406 (2018).
- [95] B. Vermersch, A. Elben, M. Dalmonte, J. I. Cirac and P. Zoller, Unitary n -designs via random quenches in atomic Hubbard and spin models: Application to the measurement of Rényi entropies, *Phys. Rev. A* **97**, 023604 (2018).
- [96] T. Brydges, A. Elben, P. Jurcevic, B. Vermersch, C. Maier, B. P. Lanyon, P. Zoller, R. Blatt, and C. F. Roos, Probing Rényi entanglement entropy via randomized measurements, *Science* **364**, 260 (2019).
- [97] A. Lukin, M. Rispoli, R. Schittko, M. E. Tai, A. M. Kaufman, S. Choi, V. Khemani, J. Leonard, and M. Greiner, Probing entanglement in a many-body localized system, *Science*, **364**, 6437 (2019).
- [98] L. Amico, R. Fazio, A. Osterloh, and V. Vedral, Entanglement in Many-Body Systems, *Rev. Mod. Phys.* **80**, 517 (2008); P. Calabrese, J. Cardy, and B. Doyon, Entanglement entropy in extended quantum systems, *J. Phys. A* **42**, 500301 (2009); N. Laflorencie, Quantum entanglement in condensed matter systems, *Phys. Rep.* **643**, 1 (2016).
- [99] E. H. Lieb and D. W. Robinson, The finite group velocity of quantum spin systems, *Commun. Math. Phys.* **28**, 251 (1972).
- [100] L. Bonnes, F. H. L. Essler, and A. M. Läuchli, “Light-Cone” Dynamics After Quantum Quenches in Spin Chains, *Phys. Rev. Lett.* **113**, 187203 (2014).
- [101] M. Fagotti and P. Calabrese, Evolution of entanglement entropy following a quantum quench: Analytic results for the XY chain in a transverse magnetic field. *Phys. Rev. A* **78**, 010306 (2008).
- [102] V. Eisler and I. Peschel, Entanglement in a periodic quench, *Ann. Phys. (Berlin)* **17**, 410 (2008).
- [103] M. G. Nezhadhighi and M. A. Rajabpour, Entanglement dynamics in short and long-range harmonic oscillators, *Phys. Rev. B* **90**, 205438 (2014).
- [104] M. Kormos, L. Bucciattini, and P. Calabrese, Stationary entropies after a quench from excited states in the Ising chain, *EPL* **107**, 40002 (2014).
- [105] L. Bucciattini, M. Kormos, and P. Calabrese, Quantum quenches from excited states in the Ising chain, *J. Phys. A* **47**, 175002 (2014).
- [106] M. Collura, M. Kormos, and P. Calabrese, Stationary entropies following an interaction quench in 1D Bose gas, *J. Stat. Mech.* P01009 (2014).
- [107] E. Bianchi, L. Hackl, and N. Yokomizo, Linear growth of the entanglement entropy and the Kolmogorov-Sinai rate, *JHEP* **03** (2018) 25.
- [108] L. Hackl, E. Bianchi, R. Modak, and M. Rigol, Entanglement production in bosonic systems: Linear and logarithmic growth, *Phys. Rev. A* **97**, 032321 (2018).
- [109] A. S. Buyskikh, M. Fagotti, J. Schachenmayer, F. Essler, and A. J. Daley, Entanglement growth and correlation spreading with variable-range interactions in spin and fermionic tunnelling models, *Phys. Rev. A* **93**, 053620 (2016).
- [110] I. Frerot, P. Naldesi, and T. Roscilde, Multi-speed prethermalization in spin models with power-law decaying interactions, *Phys. Rev. Lett.* **120**, 050401 (2018).
- [111] M. R. M. Mozaffar and A. Mollabashi, Entanglement evolution in Lifshitz-type scalar theories, *JHEP* **01** (2019) 137.
- [112] K.-Y. Kim, M. Nishida, M. Nozaki, M. Seo, Y. Sugimoto, and A. Tomiya, Entanglement after quantum quenches in Lifshitz scalar theories, *J. Stat. Mech.* (2019) 093104.
- [113] G. Di Giulio, R. Arias, and E. Tonni, Entanglement Hamiltonians in 1D free lattice models after a global quantum quench, *J. Stat. Mech.* (2019) 123103.
- [114] L. Piroli, E. Vernier, P. Calabrese, and B. Pozsgay, Integrable quenches in nested spin chains I: the exact steady states, *J. Stat. Mech.* (2019) 063103.
- [115] L. Piroli, E. Vernier, P. Calabrese, and B. Pozsgay, Integrable quenches in nested spin chains II: fusion of boundary transfer matrices, *J. Stat. Mech.* (2019) 063104.
- [116] M. Mestyán, B. Bertini, L. Piroli, and P. Calabrese, Exact solution for the quench dynamics of a nested integrable system, *J. Stat. Mech.* (2017) 083103.
- [117] R. Modak, L. Piroli, and P. Calabrese, Correlation and entanglement spreading in nested spin chains, *J. Stat. Mech.* (2019) 093106.
- [118] G. De Chiara, S. Montangero, P. Calabrese, and R. Fazio, Entanglement Entropy dynamics in Heisenberg chains, *J. Stat.*

- Mech.* (2006) P03001.
- [119] H. Kim and D. A. Huse, Ballistic Spreading of Entanglement in a Diffusive Nonintegrable System, *Phys. Rev. Lett.* **111**, 127205 (2013).
 - [120] A. Nahum, J. Ruhman, S. Vijay, and J. Haah, Quantum Entanglement Growth Under Random Unitary Dynamics, *Phys. Rev. X* **7**, 031016 (2017).
 - [121] A. Laeuchli and C. Kollath, Spreading of correlations and entanglement after a quench in the Bose-Hubbard model, *J. Stat. Mech.* P05018 (2008).
 - [122] A. Nahum, S. Vijay, and J. Haah, Operator Spreading in Random Unitary Circuits, *Phys. Rev. X* **8**, 021014 (2018).
 - [123] A. Nahum, J. Ruhman, and D. A. Huse, Dynamics of entanglement and transport in 1D systems with quenched randomness, *Phys. Rev. B* **98**, 035118 (2018).
 - [124] C. von Keyserlingk, T. Rakovszky, F. Pollmann, and S. Sondhi, Operator hydrodynamics, OTOCs, and entanglement growth in systems without conservation laws, *Phys. Rev. X* **8**, 021013 (2018).
 - [125] M. Kormos, M. Collura, G. Takács, and P. Calabrese, Real time confinement following a quantum quench to a non-integrable model, *Nature Phys.* **13**, 246 (2017).
 - [126] M. Collura, M. Kormos, G. Takacs, Dynamical manifestation of Gibbs paradox after a quantum quench, *Phys. Rev. A* **98**, 053610 (2018).
 - [127] V. Alba, Entanglement and quantum transport in integrable systems, *Phys. Rev. B* **97**, 245135 (2018).
 - [128] B. Bertini, M. Fagotti, L. Piroli, and P. Calabrese, Entanglement evolution and generalised hydrodynamics: noninteracting systems, *J. Phys. A* **51**, 39LT01 (2018).
 - [129] V. Alba, B. Bertini, and M. Fagotti, Entanglement evolution and generalised hydrodynamics: interacting integrable systems, *SciPost Phys.* **7**, 005 (2019).
 - [130] A. Bastianello, V. Alba, and J.-S. Caux, Generalized Hydrodynamics with Space-Time Inhomogeneous Interactions, *Phys. Rev. Lett.* **123**, 130602 (2019).
 - [131] J. Dubail, J.-M. Stéphan, J. Viti, P. Calabrese, Conformal field theory for inhomogeneous one-dimensional quantum systems: the example of non-interacting Fermi gases, *SciPost Phys.* **2**, 002 (2017).
 - [132] M. Mestyan and V. Alba, Molecular dynamics simulation of entanglement spreading in generalized hydrodynamics [arXiv:1905.03206](https://arxiv.org/abs/1905.03206).
 - [133] X. Cao, A. Tilloy, and A. De Luca, Entanglement in a fermion chain under continuous monitoring, *SciPost Phys.* **7**, 024 (2019).
 - [134] P. Ruggiero, Y. Brun, and J. Dubail, Conformal field theory on top of a breathing one-dimensional gas of hard core bosons, *SciPost Phys.* **6**, 051 (2019).
 - [135] B. Bertini, E. Tartaglia, and P. Calabrese, Entanglement and diagonal entropies after a quench with no pair structure, *J. Stat. Mech.* (2018) 063104.
 - [136] A. Bastianello and P. Calabrese, Spreading of entanglement and correlations after a quench with intertwined quasiparticles, *SciPost Phys.* **5**, 033 (2018).
 - [137] A. Bastianello and M. Collura, Entanglement spreading and quasiparticle picture beyond the pair structure, *SciPost Phys.* **8**, 045 (2020).
 - [138] V. Alba and P. Calabrese, Quench action and Renyi entropies in integrable systems, *Phys. Rev. B* **96**, 115421 (2017).
 - [139] V. Alba and P. Calabrese, Renyi entropies after releasing the Néel state in the XXZ spin-chain, *J. Stat. Mech.* (2017) 113105.
 - [140] V. Alba, Towards a generalized hydrodynamics description of Renyi entropies in integrable systems *Phys. Rev. B* **99**, 045150 (2019).
 - [141] M. Mestyan, V. Alba, and P. Calabrese, Renyi entropies of generic thermodynamic macrostates in ntegrable systems, *J. Stat. Mech.* (2018) 083104.
 - [142] A. Coser, E. Tonni, and P. Calabrese, Entanglement negativity after a global quantum quench, *J. Stat. Mech.* P12017 (2014).
 - [143] V. Alba and P. Calabrese, Quantum information dynamics in multipartite integrable systems, *EPL* **126**, 60001 (2019).
 - [144] J. Kudler-Flam, M. Nozaki, S. Ryu, and M. T. Tan, Quantum vs. classical information: operator negativity as a probe of scrambling, *JHEP* **01** (2020) 31.
 - [145] V. Alba and F. Carollo, Spreading of correlations in Markovian open quantum systems, [arXiv:2002.09527](https://arxiv.org/abs/2002.09527)
 - [146] S. Maity, S. Bandyopadhyay, S. Bhattacharjee, and A. Dutta, Growth of mutual information in a quenched one-dimensional open quantum manybody system, [arXiv:2001.09802](https://arxiv.org/abs/2001.09802).
 - [147] S. Chapman, J. Eisert, L. Hackl, M. P. Heller, R. Jefferson, H. Marrochio, R. C. Myers, *SciPost Phys.* **6**, 034 (2019).
 - [148] S. Sachdev, *Quantum Phase Transitions*, Cambridge University Press (2001).
 - [149] K. Sengupta, S. Powell, and S. Sachdev, Quench dynamics across quantum critical points, *Phys. Rev. A* **69**, 053616 (2004).
 - [150] O. A. Castro-Alvaredo, M. Lencses, I. M. Szecsenyi and J. Viti, Entanglement dynamics after a quench in Ising field theory: a branch point twist field approach, *JHEP* **12** (2019) 079.
 - [151] P. P. Mazza, J.-M. Stéphan, E. Canovi, V. Alba, M. Brockmann, and M. Haque, Overlap distributions for quantum quenches in the anisotropic Heisenberg chain, *J. Stat. Mech.* (2016) P013104.
 - [152] I. Peschel, Calculation of reduced density matrices from correlation functions, *J. Phys. A* **36**, L205 (2003).
 - [153] I. Peschel, Entanglement in solvable many-particle models, *Braz. J. Phys.* **42**, 267 (2012).
 - [154] I. Peschel and V. Eisler, Reduced density matrices and entanglement entropy in free lattice models, *J. Phys. A* **42**, 504003 (2009).

- [155] V. Eisler and Z. Racz, Full Counting Statistics in a Propagating Quantum Front and Random Matrix Spectra, *Phys. Rev. Lett.* **110**, 060602 (2013).
- [156] P. Calabrese, P. Le Doussal, and S. N. Majumdar, Random matrices and entanglement entropy of trapped Fermi gases, *Phys. Rev. A* **91**, 012303 (2015).
- [157] C. B. Mendl and H. Spohn, Searching for the Tracy-Widom distribution in nonequilibrium processes, *Phys. Rev. E* **93**, 060101 (2016).
- [158] J. Viti, J.-M. Stephan, J. Dubail and M. Haque, Inhomogeneous quenches in a free fermionic chain: Exact results, *EPL* **115**, 40011 (2016);
N. Allegra, J. Dubail, J.-M. Stephan and J. Viti, Inhomogeneous field theory inside the arctic circle, *J. Stat. Mech.* (2016) 053108.
- [159] P. Le Doussal, S. N. Majumdar and G. Schehr, Multicritical edge statistics for the momenta of fermions in nonharmonic traps, *Phys. Rev. Lett.* **121**, 030603 (2018).
- [160] J.-M. Stéphan, Free fermions at the edge of interacting systems, *SciPost Phys.* **6**, 057 (2019).
- [161] J. S. Cotler, M. P. Hertzberg, M. Mezei, and M. T. Mueller, Entanglement Growth after a Global Quench in Free Scalar Field Theory, *JHEP* **11**, 166 (2016).
- [162] I. Peschel and M.-C. Chung, Density matrices for a chain of oscillators, *J. Phys. A* **32**, 8419 (1999).
- [163] M. Takahashi, Thermodynamics of one-dimensional solvable models, Cambridge University Press (1999).
- [164] M. Gaudin, La fonction d'onde de Bethe, Masson (1983);
M. Gaudin (translated by J.-S. Caux), The Bethe wave function, Cambridge University Press (2014).
- [165] M. Brockmann, B. Wouters, D. Fioretto, J. De Nardis, R. Vlijm and J.-S. Caux, Quench action approach for releasing the Néel state into the spin-1/2 XXZ chain, *J. Stat. Mech.* (2014) P12009.
- [166] B. Wouters, J. De Nardis, M. Brockmann, D. Fioretto, M. Rigol, and J.-S. Caux, Quenching the Anisotropic Heisenberg Chain: Exact Solution and Generalized Gibbs Ensemble Predictions, *Phys. Rev. Lett.* **113**, 117202 (2014).
- [167] B. Pozsgay, M. Mestyán, M. A. Werner, M. Kormos, G. Zarand, G. Takács, Correlations after quantum quenches in the XXZ spin chain: Failure of the Generalized Gibbs Ensemble, *Phys. Rev. Lett.* **113**, 117203 (2014).
- [168] L. Piroli, B. Pozsgay, and E. Vernier, From the quantum transfer matrix to the quench action: the Loschmidt echo in XXZ Heisenberg spin chains, *J. Stat. Mech.* (2017) 23106.
- [169] M. Mestyán, B. Pozsgay, G. Takács, and M. A. Werner, Quenching the XXZ spin chain: quench action approach versus generalized Gibbs ensemble, *J. Stat. Mech.* (2015) P04001.
- [170] V. Alba, and P. Calabrese, The quench action approach in finite integrable spin chains, *J. Stat. Mech.* (2016) 043105.
- [171] L. Piroli, E. Vernier, and P. Calabrese, Exact steady states for quantum quenches in integrable Heisenberg spin chains, *Phys. Rev. B* **94**, 054313 (2016).
- [172] L. Piroli, E. Vernier, P. Calabrese, and M. Rigol, Correlations and diagonal entropy after quantum quenches in XXZ chains, *Phys. Rev. B* **95**, 054308 (2017).
- [173] L. Piroli, B. Pozsgay, and E. Vernier, What is an integrable quench?, *Nucl. Phys. B* **925**, 362 (2017).
- [174] V. Alba, L. Tagliacozzo, and P. Calabrese, Entanglement entropy of two disjoint blocks in critical Ising models, *Phys. Rev. B* **81**, 060411 (2010).
- [175] J. De Nardis, L. Piroli, and J.-S. Caux, Relaxation dynamics of local observables in integrable systems, *J. Phys. A* **48**, 43FT01 (2015).
- [176] J. De Nardis and J.-S. Caux, Analytical expression for a post-quench time evolution of the one-body density matrix of one-dimensional hard-core bosons, *J. Stat. Mech.* (2014) P12012.
- [177] S. R. White and A. E. Feiguin, Real-Time Evolution Using the Density Matrix Renormalization Group, *Phys. Rev. Lett.* **93**, 076401 (2004).
- [178] A. J. Daley, C. Kollath, U. Schollock, and G. Vidal, Time-dependent density-matrix renormalization-group using adaptive effective Hilbert spaces, *J. Stat. Mech.* (2004) P04005.
- [179] U. Schollwöck, The density-matrix renormalization group in the age of matrix product states, *Ann. Phys.* **326**, 96 (2011).
- [180] ITensor, Intelligent Tensor C ++ library <http://itensor.org>.
- [181] A. De Luca, M. Collura, and J. De Nardis, Nonequilibrium spin transport in integrable spin chains: Persistent currents and emergence of magnetic domains, *Phys. Rev. B* **96**, 020403(R) (2017).
- [182] T. Zhou and A. W.W. Ludwig, On the diffusive scaling of Rényi entanglement entropy, [arXiv:1911.12384](https://arxiv.org/abs/1911.12384).
- [183] M. Znidaric, Entanglement growth in diffusive systems, [arXiv:1912.03645](https://arxiv.org/abs/1912.03645).
- [184] T. Rakovszky, F. Pollmann, and C. W. von Keyserlingk, Sub-ballistic Growth of Renyi Entropies due to Diffusion, *Phys. Rev. Lett.* **122**, 250602 (2019);
T. Rakovszky, C. W. von Keyserlingk, and F. Pollmann, Entanglement growth after inhomogeneous quenches *Phys. Rev. B* **100**, 125139 (2019).
- [185] V. Khemani, A. Vishwanath, and D. A. Huse, Operator Spreading and the Emergence of Dissipative Hydrodynamics under Unitary Evolution with Conservation Laws, *Phys. Rev. X* **8**, 031057 (2018).
- [186] M. Collura, A. De Luca, and J. Viti, Analytic solution of the domain-wall nonequilibrium stationary state, *Phys. Rev. B* **97**, 081111 (2018).
- [187] G. Misguich, K. Mallick, and P. L. Krapivsky, Dynamics of the spin-1/2 Heisenberg chain initialized in a domain-wall state, *Phys. Rev. B* **96**, 195151 (2017).
- [188] M. Collura, A. De Luca, P. Calabrese, and J. Dubail, Domain-wall melting in the spin-1/2 XXZ spin chain: emergent Luttinger liquid with fractal quasi-particle charge, [arXiv:2001.04948](https://arxiv.org/abs/2001.04948).
- [189] V. Alba and F. Heidrich-Meisner, Entanglement spreading after a geometric quench in quantum spin chains *Phys. Rev.*

- [B 90, 075144 \(2014\)](#).
- [190] M. Gruber and V. Eisler, Magnetization and entanglement after a geometric quench in the XXZ chain, [Phys. Rev. B 99, 174403 \(2019\)](#).
- [191] T. LeBlond, K. Mallayya, L. Vidmar, and M. Rigol, Entanglement and matrix elements of observables in interacting integrable systems, [Phys. Rev. E 100, 062134 \(2019\)](#).